Comprehensive Summaries of Uppsala Dissertations
from the Faculty of Science and Technology 942

ALD Buffer Layer Growth and Interface Formation on $Cu(In,Ga)Se_2$ Solar Cell Absorbers

BY

JAN STERNER

ACTA UNIVERSITATIS UPSALIENSIS
UPPSALA 2004

Dissertation presented at Uppsala University to be publicly examined in Polhemssalen, Ångströmslaboratoriet, Uppsala, Friday, March 12, 2004 at 09:30 for the degree of Doctor of Philosophy. The examination will be conducted in English.

Abstract

Sterner, J. 2004. ALD Buffer Layer Growth and Interface Formation on $Cu(In,Ga)Se_2$ Solar Cell Absorbers. Acta Universitatis Upsaliensis. *Comprehensive Summaries of Uppsala Dissertations from the Faculty of Science and Technology* 942. 51 pp. Uppsala.
ISBN 91-554-5883-1

$Cu(In,Ga)Se_2$ (CIGS) thin film solar cells contain a thin layer of CdS. To avoid toxic heavy-metal-containing waste in the module production the development of a cadmium-free buffer layer is desirable. This thesis considers alternative Cd-free buffer materials deposited by Atomic Layer Deposition (ALD). Conditions of the CIGS surface necessary for ALD growth are investigated and the heterojunction interface is characterized by band alignment studies of ZnO/CIGS and In_2S_3/CIGS interfaces. The thesis also includes investigations on the surface modification of the CIGS absorber by sulfurization.

According to ALD theory the growth process is limited by surface saturated reactions. The ALD growth on CIGS substrates shows nucleation failure and generally suffers from surface contaminations of the CIGS layer. The grade of growth disturbance varies for different ALD precursors. The presence of surface contaminants is related to the substrate age and sodium content. Improved growth behavior is demonstrated by different pretreatment procedures.

The alignment of the energy bands in the buffer/absorber interface is an important parameter for minimization of the losses in a solar cell. The valence band and conduction band offsets was determined by *in situ* X-ray and UV photoelectron spectroscopy during layer by layer formation of buffer material. The conduction band offset (ΔE_c) should be small but positive for optimal solar cell electrical performance according to theory. The conduction band offset was determined for the ALD ZnO/CIGS interface (ΔE_c = -0.2 eV) and the ALD In_2S_3/CIGS interface (ΔE_c = -0.25 eV).

A high temperature process for bandgap grading and a low temperature process for surface passivation by post deposition sulfurization in H_2S were investigated. It is concluded that the high temperature sulfurization of $CuIn_{(1-x)}Ga_xSe_2$ leads to phase separation when x>0. The low temperature process did not result in enhanced device performance.

Keywords: thin film, Cu(In,Ga)Se2, CIGS, chalcopyrite, ALD, sulfurization, buffer layer, XPS, UPS, electron spectroscopy, band alignment, atomic layer deposition

Jan Sterner, Department of Engineering Sciences, Box 534, Uppsala University, SE-751 21 Uppsala, Sweden

ISSN 1104-232X
ISBN 91-554-5883-1
urn:nbn:se:uu:diva-4009 (http://urn.kb.se/resolve?urn=urn:nbn:se:uu:diva-4009)

Till min familj

Publications

This thesis is based on the following publications, which will be referred to in the text by their Roman numerals.

I. J. Sterner, J. Kessler, M. Bodegård, & L. Stolt. *Atomic Layer Epitaxy Growth of ZnO Buffer Layers in Cu(In,Ga)Se_2 Solar Cells*, in proceedings of the 2nd World Conference on Photovoltaic Energy Conversion, Vienna. (1998) 1145-1148.

II. J. Sterner, T. W. Matthes, J. Kessler, J. Lu, J. Keränen, E. Olsson, and L. Stolt. *Sulfurization of thin film solar cell absorbers*, in proceedings of the 16th European Photovoltaic Solar Energy Conference and Exhibition, Glasgow. (2000) 771-774.

III. J. Keränen, J. Lu, J. Barnard, J. Sterner, J. Kessler, L. Stolt, T. W. Matthes, and E. Olsson, *Effect of sulfurization on the microstructure of chalcopyrite thin-film absorbers*. Thin Solid Films, 387 (2001) 80-82.

IV. J. Sterner, J. Kessler, & L. Stolt. *XPS instrument coupled with ALCVD reactor for investigation of film growth*. Journal of Vacuum Science & Technology A (Vacuum, Surfaces, and Films), 20 (2002) 278-284.

V. J. Sterner, C. Platzer-Björkman, and L. Stolt. *XPS/UPS monitoring of ALCVD ZnO growth on Cu(In,Ga)Se_2 absorbers*, in proceedings of the 17th European Photovoltaic Solar Energy Conference and Exhibition, Munich. (2001) 1118-1121.

VI. J. Sterner, J. Malmström, and L. Stolt. *Study on ALD In_2S_3/Cu(In,Ga)Se_2 interface formation*, submitted to Progress in Photovoltaics.

VII. J. Sterner, J. Kessler, J. Keränen, M. Edoff, T. W. Matthes, A. Rockett, and L. Stolt. *Influence of Ga on sulfurization of Cu(In,Ga)Se_2 thin films*, submitted to Thin Solid Films.

The contribution by the author to the papers included in the thesis is as follows:

I. All experimental work*, major part of evaluation and writing.

II. All experimental work*, major part of evaluation and writing.

III. Major part of experimental work*, no part of analysis work and minor part of writing.

IV. Part of conceptual and design work. All experimental work, major part of evaluation and writing.

V. Part of experimental work*, evaluation and writing.

VI. Major part of experimental work*, part of evaluation and writing.

VII. All experimental work* except SIMS and TEM studies. Part of evaluation and writing.

* Preparation of $CuInSe_2$, $CuGaSe_2$, and $Cu(In,Ga)Se_2$ absorbers used in all papers, is done by coworkers of the author.

Table of contents

1 Introduction

Today one of our major challenges is to find a sustainable supply of electrical energy. Our current energy system is to a large extent based on the use of fossil fuels. Emission of green-house gases is supposed to lead to global warming and acidfication.

Besides the negative environmental impact our energy demand often induces political instability like the control of oil and gas reserves and the use of nuclear power. In order to be robust, our energy infrastructure should be distributed and close to the source. The photovoltaic source of energy, i.e. solar irradiation, has the advantage of being widely distributed over the world, although the largest demand does not always correlate with the supply. The solar irradiation impinging on the earth's surface is not a limiting factor and supersedes our needs by far.

Future design of our energy system will be a combination of different alternatives. Solar cells never will or can constitute the only solution. Common for the alternatives are a few requirements. The resource must be sustainable and the price must be in level with today's cost of energy. Furthermore we must have a technology to scale up and produce this system. Solar cell technology is about to meet all of these standards.

1.1 Solar Cells

The basic task of a solar cell is to absorb incoming light, create electron-hole pairs and transfer them to the device contacts for transport in an external circuit. The depletion region of a pn junction is well suited to serve this function. The ability to absorb light is defined mainly by the band shape and the width of the bandgap, E_g. The separation and transport of the photo-generated free carriers are supported by the built-in electric field formed by the junction. A transparent conductive oxide (TCO) is normally used for current collection in the front and a metal contact in the back of solar cells.

Crystalline silicon has become the dominant solar cell technology mostly due to its volume application in microelectronics. The solar cells that are commercially available today are made from solar grade silicon rejected by the microelectronics industry. Although high efficiencies are achieved with crystalline Si, this technology is not expected to become a low cost alternative. One reason is the poor light absorption of Si which results in a cell design with thick absorbers and high material consumption. The silicon must be very pure and perfectly crystalline for photo-generated carriers to reach the contacts. The device is based on a homojunction, commonly formed by diffusion of dopants into p-type silicon wafer.

Efficient solar cells can be made by thin film technology. By use of semiconductor material with high absorption, a film thickness of a few μm is enough for an effective capture of the light. There are a number of different absorber materials. Most common today are devices based on amorphous silicon, normally deposited by chemical vapor deposition (CVD). These devices have reached an unstabilized efficiency of 13.1%. More complex compounds also are utilized in heterojunction devices, such as CdTe, CdS/CuS, CdS/$CuInSe_2$ and others. CdTe cells are reported at a maximum efficiency of 16.5%. [1]

Thin film technology benefits from low material consumption and low price compared to crystalline silicon cells. The up scaling of this technology from the single solar cell to the large area module is straight forward since many cells can be interconnected from material deposited on one substrate in the form of stacked film layers. Compared to the crystalline material, thin film solar cells can be manufactured with less input of energy. This will shorten the energy pay back time, defined as the time it takes until the photo-generated energy output equals the energy that was consumed to produce the device.

Specific advantages of the $CuInSe_2$ alloy are its wide compositional tolerance and high optical absorption in the visible spectrum. One major drawback for mass production is the limited extraction rate of indium from mining.

2 Cu(In,Ga)Se$_2$ solar cells

2.1 Device structure

The Cu(In,Ga)Se$_2$ cell device in its standard design consists of five thin layers supported by a glass substrate. The structure is illustrated in Figure 1, where light is coming from above. The Cu(In,Ga)Se$_2$ layer is moderately p-doped while the CdS and also the ZnO layers constitute the n-doped part of the pn-junction. The Cu(In,Ga)Se$_2$ and CdS films are doped by intrinsic defects in the material while the top ZnO layer is intentionally doped with Al. Between the CdS and doped ZnO layers is an undoped layer of ZnO. The separated carriers from the electron-hole pairs are collected at the electric contacts in each end of the cell: ZnO:Al in the front and Mo in the back. The laboratory scale cells are equipped with a Ni/Al/Ni grid for current collection on the front contact.

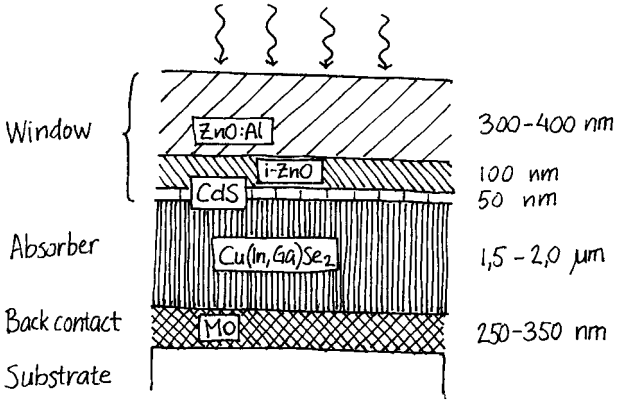

Figure 1: Device structure of a Cu(In,Ga)Se$_2$ solar cell.

In the following sections each layer will be described and certain properties will be enlightened which are of importance for the thesis. Special attention will be paid to the buffer layer and its interface with the absorber layer.

2.1.1 Substrate and back contact

The baseline Cu(In,Ga)Se$_2$ solar cell [2] uses a soda lime glass substrate, originally because it was available and cheap, but later on it has been realized that the sodium content of the glass plays an important role and improves the device performance. Onto the cleaned glass substrate a back contact layer of molybdenum is sputter deposited. Other materials for back contact deposition have been investigated but Mo is found superior for various reasons. One reason is the diffusion of Na through the Mo film into the Cu(In,Ga)Se$_2$ which improves the crystalline quality of the layer [3]. For experimental purpose, an additional Al_2O_3 layer acting as a diffusion barrier on the glass substrate can eliminate the Na diffusion into the absorber and be used to study the influence of Na. Low film porosity makes the Atomic Layer Deposition (ALD) process suitable for barrier deposition and highly effective barriers are achieved by ALD Al_2O_3 deposited on glass at 300 °C. Mo is sputtered

directly on the barrier layer. This type of substrate will be referred to as barrier substrate in this work.

2.1.2 Absorber layer

The Cu(In,Ga)Se_2 compound belongs to the semiconducting I-III-VI_2 materials family that crystallize in the tetragonal chalcopyrite structure. Chalcopyrite is another name for copper iron sulfide ($CuFeS_2$), a common copper ore, which gave name to these materials. An interesting property of the semiconducting chalcopyrites in general and Cu(In,Ga)Se_2 in particular is that E_g can be varied, for instance by varying the amount of Ga. The optimal bandgap for a solar cell with respect to the solar spectrum is around 1.4 eV [4]. The bandgap of $CuInSe_2$ is 1.04 eV and 1.68 eV for $CuGaSe_2$ while the bandgap of the alloys Cu(In,Ga)Se_2 lies in between. A Ga/(In+Ga) ratio of 30% results in E_g at about 1.2 eV, which has been shown empirically to give the best device results. Another way to increase E_g is by replacing part of the Se for S and form Cu(In,Ga)$(Se,S)_2$. It is expected that a wider E_g will give a higher V_{oc}. At a given efficiency higher voltage and lower current is preferred, since lower current results in smaller resistive losses with $P = I^2R$. In a module with several interconnected cells an increased voltage is of interest. Since a higher voltage corresponds to a lower current for the same power, a superior design of wider cells with smaller geometrical losses can be used.

Cu(In,Ga)Se_2 is evaporated onto the Mo from elemental sources. Our baseline recipe sets the Ga/(Ga+In) ratio to around 30%. In this work $CuIn_{(1-x)}Ga_xSe_2$ with x from 0 to 1 is used. Where not stated otherwise x lies between 0.3 and 0.45. Absorbers are deposited at a maximum substrate temperature of 510 °C, from resistive open boat sources in a Balzers evaporation system with source flux rates controlled by a Quadrupole Mass Spectrometer (QMS).

In Paper II, III and VI two methods are evaluated for post deposition sulfurization of coevaporated Cu(In,Ga)Se_2 absorbers, aiming for an increased bandgap (E_g) at the surface. The background and results from sulfurization experiments will be discussed further in Chapter 7.

2.1.3 Buffer layer and front contact

At the front side, current is collected by a 300-400 nm thick Al-doped ZnO layer, deposited by RF magnetron sputtering onto a 100 nm thick layer of not intentionally doped high resistive ZnO (i-ZnO). Between the Cu(In,Ga)Se_2 absorber and ZnO layers a 50 nm thick buffer layer of CdS is deposited. The role of the buffer layer is discussed in Section 2.3.

Critical parameters for the transparent conductive oxide (TCO) are the sheet resistivity and the optical transmittance. As they are inversely related to each other, an optimal value can be derived depending on the exact design of the solar cell. Single cells are normally equipped with a metal grid for carrier collection and are not so sensitive to the sheet resistance of the TCO. In a module several cells are interconnected in series and the TCO will have to carry the total current generated by the module. As a result, low sheet resistance becomes more critical in module applications. A way to measure TCO performance is the figure of merit proposed by Kessler *et al.* [5] expressed in terms of reduced current density due to optical absorption in the front contact for a given sheet resistance. Yet another interesting

parameter of the ZnO window layer is its ability to scatter the incoming sunlight and further improve absorption by prolonging its path through the absorber. Light scattering is promoted by surface roughness and quantified by measuring the film haze factor, which is defined as the ratio between diffuse and total transmittance.

2.2 Device operation

The operation of solar cells in general is thoroughly described in several books, for example Green [4] or Fonash [6]. A short description of the device operation is given here and special features that apply for the $CuInSe_2$ type of thin film solar cells. The electrical performance of a solar cell is normally characterized by current voltage (IV) measurements. A typical plot for a device under illumination and in dark is shown in Figure 2.

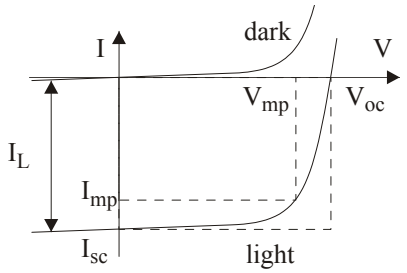

Figure 2: IV characteristics of a solar cell under dark and illuminated conditions, displaying V_{oc}, I_{sc} and maximum power point $P_{max}=V_{mp}I_{mp}$.

From IV characterization, the open circuit voltage V_{oc}, the short circuit current I_{sc}, the fill factor (*FF*) and the efficiency (η) at the maximum power working point (V_{mp}, I_{mp}) are extracted. The voltage *V*, current *I*, *FF* and η are related by Equations (1-5).

$$I = I_0(e^{qV/nkT} - 1) - I_L \tag{1}$$

I_0 is the saturation current in dark, n the diode quality factor and I_L the photogenerated current. From Equation (1) we get the I_{sc} under short circuit conditions (V = 0) according to Equation (2). Setting the current to zero in Equation (1) gives the V_{oc} according to Equation (3).

$$I_{sc} \equiv I(V = 0) = I_L \tag{2}$$

$$V_{oc} = \frac{nkT}{q}\ln\left(\frac{I_L}{I_0} + 1\right) \tag{3}$$

$$FF = \frac{V_{mp}I_{mp}}{V_{oc}I_{sc}} \tag{4}$$

$$\eta = \frac{V_{mp}I_{mp}}{P_{in}} = \frac{V_{oc}I_{sc}FF}{P_{in}} \tag{5}$$

2.2.1 Quantum efficiency

The quantum efficiency, QE(λ), is the ratio of the number of carriers collected by the solar cell to the number of incident photons at a given wavelength of the incident light. The internal QE is defined in the same way but only considers the photons that are absorbed in the device, i.e. not lost by reflection or transmission from the solar cell. From QE plots estimated values of E_g for the Cu(In,Ga)Se$_2$ layer and the window layer are extracted together with I_{sc} for the device.

2.2.2 Loss mechanisms

In a solar cell with no losses each photon striking the surface would transfer its total energy to an electron-hole pair and all carriers would maintain and transfer the absorbed energy to the device contacts and a conversion efficiency of 100% would be achieved. Losses due to transmittance through the device, relaxation losses due to excess photon energy, and carrier recombination, provide a limit for the achievable efficiency of a single junction device which is much smaller (about 30%) [4,7].

A number of different mechanisms are identified as responsible for recombination losses in a Cu(In,Ga)Se$_2$ device. In Figure 3 the locations of interface recombination (a), recombination due to traps in the depletion region (b) and in the bulk (c) are marked. The dominating recombination type for Cu(In,Ga)Se$_2$ solar cells is (b). Traps in the depletion region reduce V_{oc} and *FF*. This effect is strongest for traps at an energy level close to the middle of the bandgap. Devices with poor interface quality often show type (a) recombination as well. Devices based on ALD buffers are in some cases found to suffer from increased interface recombination. This thesis will focus on properties that influence recombination of type (a) and (b).

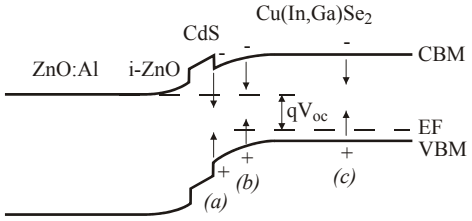

Figure 3: Qualitative band diagram for the Cu(In,Ga)Se$_2$ solar cell under illumination and open circuit conditions. Recombination types are indicated in region of occurrence: interface (a), space charge region (SCR) (b), and bulk recombination (c).

2.2.3 Band offsets

When one semiconductor material is deposited onto another a heterojunction is formed. With different workfunctions ϕ and electron affinities χ for the two types of semiconductors a built-in field will be formed in order for the Fermi level to be constant across the interface. Due to the different electron affinities a discontinuity in the conduction band will be formed. Additionally a discontinuity will appear in the valence band, which also depends on the difference in bandgaps. In this work when considering the buffer/absorber interface the conduction band offset (ΔE_C) is

regarded as positive if the conduction band minimum (CBM) of the buffer layer is above the absorber and the valence band offset (ΔE_V) as positive if the buffer valence band maximum (VBM) is above that of the absorber. Positive ΔE_C and negative ΔE_V are shown in Figure 4.

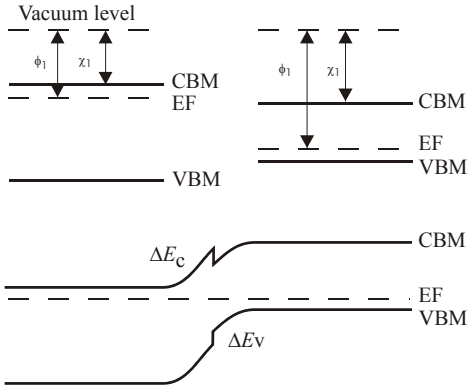

Figure 4: Energy band diagrams of buffer and absorber (upper picture) and the heterojunction formed when the layers are in contact (lower picture).

It is generally believed that ΔE_C should be zero or slightly positive, 0-0.4 eV, to minimize recombination of majority carriers at the heterojunction interface and maintain high efficiency. From a CdS/Cu(In,Ga)Se$_2$ device simulation Minemoto *et al.* [8] conclude that photogenerated carriers are blocked if $\Delta E_C > 0.4$eV resulting in a reduced *FF*, while at $\Delta E_C < 0$eV *FF* and V_{oc} are reduced due to carrier recombination at the interface. Simulation of the CdS/CuInSe$_2$ device by Turner *et al.* also results in the requirement of positive ΔE_C [9]. If ΔE_C is positive but large a spike (> 0.4eV) in the conduction band is formed and the photocurrent is suppressed. If ΔE_C is negative the open circuit voltage is limited by the built-in potential which is smaller than the bandgap of the absorber material by $-\Delta E_C$ [10].

Several groups have performed investigations to determine ΔE_V and ΔE_C for the CdS/Cu(In,Ga)Se$_2$ and CdS/Cu(In,Ga)Se$_2$ interfaces. Reported values for these and Cd-free junctions are summarized in Table 1. If the deposited buffer layer is very thin, emissions in photoelectron spectroscopy (PES) from the buffer layer and the underlying absorber material are both acquired simultaneously. The offsets in the valence band is determined by comparing VBM positions of the two layers with the binding energy for core levels (E_{CL}) from the respective layer according to Equation (6), where (CIGS) denotes the Cu(In,Ga)Se$_2$ film and (b) the buffer layer. From ΔE_V and appropriate values for the buffer and absorber bandgaps, the conduction band offset is deduced by Equation (7). Determination of the bandgap is a critical task and values are reported to differ from reference values due to interdiffusion of Se into CdS ($E_g = 2.2$ eV) [11].

$$\Delta E_{V(b/CIGS)} = (E_{CL(CIGS)} - E_{V(CIGS)}) - (E_{CL(b)} - E_{V(b)}) + \Delta E_{CL(b\text{-}CIGS)} \quad (6)$$

$$\Delta E_{C(b/CIGS)} = \Delta E_{V(b/CIGS)} + E_{g(b)} - E_{g(CIGS)} \quad (7)$$

Table 1: ΔE_V and ΔE_C for interfaces between CdS or Cd free buffers and CuInSe$_2$ or Cu(In,Ga)Se$_2$ absorber material.

Material	ΔE_V [eV]	ΔE_C [eV]	*method*	*ref.*
evap. CdS/cleav. $CuInSe_2$	-0.8 ±0.1	0.6-0.7	SXPS	[12]
CdS/$CuInSe_2$	-0.8 ±0.2	0.0 ±0.2	UPS, IPS	[11]
CdS/evap. $CuInSe_2$	-0.85	0.25	XPS, UPS	[13]
CdS/$CuInSe_2$	-1.47	-0.08	C-V	[14]
CdS/$Cu(In_{0.91},Ga_{0.09})Se_2$		0.08 ±0.10	kelvin probe	[15]
CBDZnS/3-stage $Cu(In,Ga)Se_2$	-1.0	1.4	XPS	[16]
ALD ZnS/evap. $Cu(In,Ga)Se_2$	-1.2 ±0.2	1.0 ±0.2	XPS, UPS	[17]
Zn(O,S)/evap. $Cu(In,Ga)Se_2$	-1.3 ±0.2	0.8 ±0.2	XPS, UPS	[17]
evap. ZnSe/cryst. $CuInSe_2$	-0.70 ±0.05	0.80 ±0.05	SXPS	[18]

The large values for ΔE_C determined for different Zn-S compounds is in contradiction with the high efficiencies reported for these devices. Nakada has suggested that ΔE_C is not the predominant factor for achieving high efficiency of these cells [16].

2.3 Critical role of the buffer layer

2.3.1 Efficiency gain

The standard $Cu(In,Ga)Se_2$ based solar cell contains an about 50 nm thick CdS buffer layer between the absorber layer and the transparent front contact layer, to improve efficiency. Although a number of different wide bandgap materials deposited by chemical bath deposition (CBD) have been investigated, such as (CdZn)S, Zn(OS), Zn(OH,S), ZnO, ZnS, , ZnSe, In_2S_3, $In(OH)_3$, $In(OH,S)_3$, SnO_2 etc. [19,20], best performance is achieved using the CdS buffer material. This is in contrast to the fact that a performance gain is expected for wider bandgap material due to a lower light absorption. So far the benefits of using CdS are merely observed but not completely understood. The CBD process provides an opportunity to remove contaminations of the $Cu(In,Ga)Se_2$ surface by etching with ammonia [21]. Beneficial properties of the interface are suggested to be related to the match between lattice parameters, which results in growth of CdS epilayers [22]. Passivation of the $Cu(In,Ga)Se_2$ surface is also put forward as an important feature of the CBD CdS process [21].

Another aspect is the doping of the $Cu(In,Ga)Se_2$ surface and several reports have been made on Cd diffusion [23,24]. It has been suggested that the Cu deficient top layer of the $Cu(In,Ga)Se_2$, also known as the ordered defect compound (ODC) layer, serves a possible host for Cd atoms. It is known that Cd can be used for type conversion of $CuInSe_2$ and $CuGaSe_2$ to n-type semiconductors. A buried homo-junction may be formed in the $Cu(In,Ga)Se_2$ layer, below the metallurgical interface.

The current understanding is that candidates for alternative buffer material should hold four common properties: (a) The material should be n-type in order to

form a pn junction with the absorber layer. (b) The bandgap should be wide for limited light absorption. (c) The process for deposition has a capability to passivate the surface states of the absorber layer. (d) The process and material choice of the buffer layer should provide an alignment of the conduction band with the Cu(In,Ga)Se$_2$ absorber with a ΔE_C of 0 – 0.4 eV according to Section 2.2.3. Binary sulfides, oxides and oxy-sulfides are frequently investigated as potential Cd-free buffer layers.

2.3.2 Producability

From a production point of view the CBD process step is undesirable as it constitutes the only wet process step in the whole chain, and with a dry buffer process a device might be fabricated without leaving the vacuum. On the other hand, CBD is a well-known process far ahead along the learning curve, which can safely be introduced in production. When introducing a rather young technology like ALD much effort must be spent on process and equipment development.

One reason for depositing a buffer layer at all is protection. The Cu(In,Ga)Se$_2$ absorber is sensitive and needs protection during the impact of ions when sputtering the intrinsic and doped ZnO window layers. When protected by a buffer layer the Cu(In,Ga)Se$_2$ film is also better suited for air exposure. This is of interest if the layers will be stored before the deposition of window layers is made.

2.3.3 Durability

Cu(In,Ga)Se$_2$ devices equipped with a CdS buffer exhibit excellent long-term stability. With CdS buffer, cells also show high performance directly after deposition or after a short air annealing. Alternative (Cd-free) buffer material often shows metastable properties where cells improve with extensive air annealing and/or light soaking and/or by applying a voltage bias. The gain in performance is normally lost after some time. Nakada *et al.* [25] have reported on light soaking effects for ZnS buffers and show saturated light soaking and reverse effect in darkness. Light soaking effects are suggested to be related to the Cu(In,Ga)Se$_2$ surface primarily and not to changes of the ZnO layer [26].

From DLTS measurements it is suggested that defect relaxation, trapping and detrapping of minority carriers is affected by air annealing [27] and trap assisted tunneling of carriers by light soaking [28].

3 Motivation for this work

3.1 The ALD process

As a dry, scalable and low vacuum method the ALD process constitutes a promising candidate for buffer layer formation. The method is capable of gentle film deposition well suited for the sensitive $Cu(In,Ga)Se_2$ surface. As the buffer layer is very thin it is of importance that the film is fabricated uniformly and without voids. An inherent property of the ALD process is highly conformal coating even for very thin films. Limited work has been reported on different buffer materials deposited by ALD. The CBD process on the other hand is well known and many critical aspects of the chemistry during CBD of CdS have been suggested, such as etching or doping of the $Cu(In,Ga)Se_2$ surface. In order to fully replace the CBD process, the understanding and control of the surface chemistry and possible doping effects during ALD growth might prove to be very important. ALD growth behavior as a function of different pretreatments, chemistry of the reactions and reaction paths at the $Cu(In,Ga)Se_2$ surface are research areas not yet covered.

3.2 Replacement of Cd in $Cu(In,Ga)Se_2$ solar cells

The contradiction of using heavy metals in environmentally benign energy systems and the hazardous handling of cadmium during manufacturing will probably force a $Cu(In,Ga)Se_2$ solar cell industry to find a replacement for the CdS buffer material. Besides environmental reasons, the replacement of CdS by buffer material of larger bandgap is motivated by the reduced light absorption of the window layers. The current loss of a $Cu(In,Ga)Se_2$ device caused by the CdS film is estimated to be in the order of 1 mA/cm^2 [29]. Under short circuit conditions the total current density (J_{sc}) is about 35 mA/cm^2 in a state-of-the-art $Cu(In,Ga)Se_2$ solar cell.

3.3 Band alignment studies

The ΔE_C for the $CdS/Cu(In,Ga)Se_2$ interface has been investigated in several studies and found to be within the suggested limits for optimal electrical function. In the case of Cd-free alternatives very little work has been done to investigate energy band alignment. The determination of these offsets strongly motivates the setup for *in vacuo* analysis by photoelectron spectroscopy (PES) of the ALD buffer/$Cu(In,Ga)Se_2$ interface formation.

Improved performance of the $Cu(In,Ga)Se_2$ device is expected by bandgap grading at the front. The bandgap is increased either by raising the conduction band or by lowering of the valence band edge. This modification however cannot be performed without consideration of the buffer layer properties in order to maintain the energy band alignments. The potential application of the *in vacuo* setup described in this work is the formation and optimization of the absorber grading and buffer layer.

4 Analytical tools

4.1 Compositional analysis

Among the tools for compositional determination, X-ray photoelectron spectroscopy (XPS) is used for investigations of the surface and methods like EDX and SIMS are used for examinations of the bulk composition. In this work surface properties are of primary interest for the ALD processes, while bulk analysis tools were mainly used for sulfur grading experiments.

XPS is a surface sensitive tool for chemical analysis, also called ESCA (electron spectroscopy for chemical analysis). Limited by the escape depth of electrons, spectroscopic information is only acquired for the outermost atomic layers. Identification of elements present in the sample and their chemical state is made directly from the kinetic energy of the ejected photoelectrons by Equation (8).

$$E_K = h\nu - E_B \tag{8}$$

where hν is the photon energy of the excitation source and E_B represent the binding energy of the level from which the electron was ejected. Kinetic energies are also determined for electrons emitted in Auger transitions. For a given excitation energy, the kinetic energies of both emitted core level electrons $E_K(i)$ and of emitted Auger electrons $E_K(jkl)$ can be acquired. Their difference, the Auger parameter,

$$\alpha = E_K(jkl) - E_K(i) \tag{9}$$

is calculated in order to indicate chemical changes without the problem of determining a reference level and substrate charging. Normally the modified Auger parameter

$$\alpha' = \alpha + h\nu = E_K(jkl) + E_B(i) > 0 \tag{10}$$

is used for convenience since it is always larger than zero. XPS provides a powerful tool to trace chemical shifts, for example as the result of a pre-treatment of the absorber surface. Most of the XPS work was done on a Leybold-Heraeus LHS-10 spectrometer, equipped with a dual anode X-ray tube, generating non-monochromatic X-rays at 1253.6 eV (Mg) and 1486.6 eV (Al), and a hemispherical electron energy analyzer. In addition to the X-ray source this system has a He lamp for generation of ultraviolet light. He I (21.21 eV) and He II (40.8 eV) emissions are used to perform Ultraviolet Photoelectron Spectroscopy (UPS). The physics of the technique is the same as XPS, the only difference being that much lower photon energies are used and the emphasis is on examining the valence band structure rather than core levels. The XPS/UPS system has frequently been used for the characterization of absorber layer surfaces. To gain knowledge of the ALD growth process, the XPS/UPS analyzer was *in vacuo* connected to the ALD reactor. In Chapter 6 results and experiences from this study are summarized.

High-resolution micrographs of film surfaces and cross sections were acquired by Scanning Electron Microscopy (SEM). In this work most pictures were made with a LEO 1550, FEG-SEM, which makes use of a Field Emission Gun to create a

well-focused electron beam. The SEM instruments used in this work were equipped with Energy Dispersive X-ray spectroscopy (EDX) for compositional analysis.

Secondary Ion Mass Spectroscopy (SIMS) is a method for tracing elements throughout a film and gives a compositional profile of the layer. Material is removed by sputtering and analyzed by a mass spectrometer. This method is limited by the cross sensitivity between elements and intermixing of thin layers. The method does not give information about the chemical state. Ion yield is dependent on the chemical environment, which makes general calibration difficult. SIMS studies were used to characterize $Cu(In,Ga)Se_2$ absorber films after sulfurization processes.

4.2 Structural analysis

The tools for structural analysis can be divided into microscopic and macroscopic level. Structural information on the overall properties of a thin film is acquired by X-ray diffraction (XRD) while information from single grains is achieved with Transmission Electron Microscopy (TEM).

The crystal structure, lattice constant, and the orientation in reference to the substrate surface are characterized by X-ray diffraction (XRD). Diffractograms acquired at small angles of incidence, referred to as grazing incidence or GI-XRD, enhance the surface sensitivity of the analysis and are a common tool to trace crystallographic changes of the surface as a result of surface treatment. If the samples are free from stress and homogeneous, a good estimate of the material's grain size is calculated from the peak broadening using the formula by Scheerer. XRD work was done on a Siemens D5000 diffractometer equipped with a Goebel focusing mirror and a Bruker axs D8 diffractometer.

A sophisticated tool to determine the crystal structure is Transmission Electron Microscopy (TEM). In TEM the incoming beam is made of high energetic electrons yielding a very high resolution. TEM instruments normally also are equipped with EDX. The method is capable of giving structural and compositional information on a single grain. TEM results in this work were made on a TECNAI F30 ST.

4.3 Optoelectrical characterization

Optical characterization was done on Beckman UV5240 and Lambda 900 spectrometers equipped with integrating spheres. Apart from basic reflectance and transmittance measurements of properties such as light scattering, this method is used for the optical determination of the bandgap.

Solar cell devices were characterized with current voltage (IV) measurements under simulated AM 1.5 G illumination (100 mW/cm^2). Eight cells of area 0.5 cm^2 were made from a standard substrate size of 17x50 mm. The device current and bandgap were determined by quantum efficiency (QE) measurements. QE measurements are more accurate in determining J_{sc} than standard IV measurements. This is a due to the deviation between the standard air mass (AM) 1.5 spectrum and that of the halogen lamp used in our setup.

5 Cd-free buffer layers by ALD

This chapter begins with a general description of the atomic layer deposition (ALD) process. Next the ALD ZnO and In_2S_3 processes are described and the properties of the corresponding films and their ability as buffer layers analyzed. The discussion then focuses on qualities of the $Cu(In,Ga)Se_2$ surface that are important for the ALD growth process.

5.1 Atomic Layer Deposition

The Atomic Layer Deposition process is also referred to as Atomic Layer Chemical Vapor Deposition (ALCVD) or Atomic Layer Epitaxy (ALE) when crystalline substrates are used. Despite the main use of amorphous (glass) and polycrystalline substrates ($Cu(In,Ga)Se_2$), all designations are used synonymously in the papers presented in this thesis. The process is suited for deposition of compound materials like II-VI and III-V semiconductors [30], and provides an interesting method for the fabrication of solar cell window layers. It can also be used for the deposition of elements like Mo [31] used as the backside contact in $Cu(In,Ga)Se_2$ solar cells. The fabrication of ALD deposited chalcopyrite $CuGaS_2$ at temperatures of 550-600 °C has also been reported [32]. Hence a complete $Cu(In,Ga)Se_2$ device could eventually be deposited by ALD. This method is of low interest for industrial fabrication of absorbers for reasons of the limited growth rate.

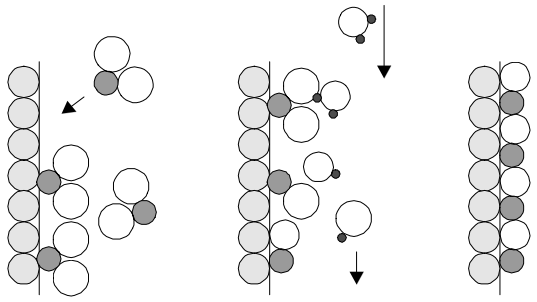

Figure 5: Growth sequence for ALD deposition of AB from AX and BY. a) AX is absorbed on the surface. Excess molecules are removed by a N_2 purge and a submonolayer is formed. b) BY reacts with the absorbed AX molecules and forms AB at the surface while reacted ligands XY are pumped away. c) The remaining monolayer of AB.

The ALD method is a modified CVD process, see Figure 5, where the reaction between for instance two reactants, here referred to as AX and BY, takes place at the substrate surface. Only one reactant is introduced in the reaction volume at a time. The process starts with a pulse of reactant AX of which a part is absorbed at the substrate surface (*a*), in this thesis referred to as a submonolayer. Remaining reactant AX is then purged by nitrogen, leaving only the molecules absorbed at the surface. Now reactant BY is pulsed (*b*). Since AX is absorbed the reaction with BY

is now limited to the surface. Another nitrogen purge clears remaining BY from the chamber and completes the ALD process cycle (*c*). As a result, the ALD reactor is capable of highly uniform film growth at a layer-by-layer resolution and the thickness is precisely controlled by the number of cycles deposited.

Under ideal conditions the submonolayer growth stops when the surface is saturated and the excess chemical is purged away. In the real world with less ideal surfaces deviations from the ideal growth process may occur. A model has been proposed by Park *et al.* to explain non ideal growth [33]. According to this, only a fraction of the free surface will be covered by AX in (a). In (b) BY will react with AX only at a fraction of the AX covered area. The deposition of partially nucleated monolayers results in a growth rate below the expected complete monolayer per reaction cycle.

In the production of $Cu(In,Ga)Se_2$ modules, three patterning steps are necessary to form and interconnect cells resulting in steps at the surface. The purpose of these scribes is to separate the back contact, the absorber layer and the window layers between adjacent cells. The resulting steps from the first two scribes are partly subjected to subsequent ALD ZnO growth. Traditional window deposition by RF sputtered ZnO exhibits poor film coverage of the steps in the absorber. The effective step coverage of the ALD process makes this process well suited for the buffer fabrication in $Cu(In,Ga)Se_2$ solar modules. As an example of the covering ability it is shown in Figure 6 how ALD ZnO completely covers the inner surface of a pinhole in a $Cu(In,Ga)Se_2$ surface.

The limited ALD growth rate is not necessarily an obstacle for this application as it is often argued that the buffer should be very thin. If implemented as a batch process the throughput is increased considerably.

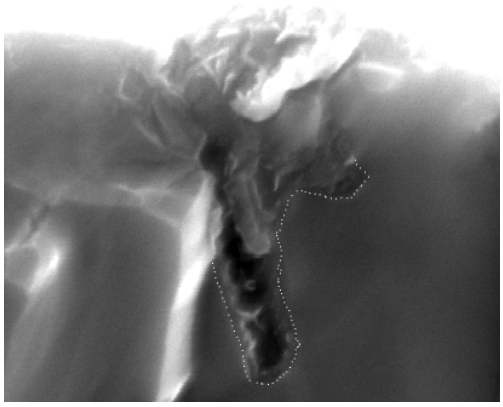

Figure 6: SEM micrograph showing ALD ZnO growth inside a pinhole at the $Cu(In,Ga)Se_2$ surface (magnification x*50k).*

The ALD processing window, which illustrate the growth rate as a function of temperature, have been reported for most compounds. Suntola [34] identifies and discusses growth mechanisms in the three temperature regions; below, within and above the process window, see Figure 7. At temperatures below the window, growth is normally slower since the activation energy is not reached (a), but it can

also be higher if condensation of reactants occurs (b). At temperatures above the window growth is slower because of desorption of the surface ligands (c) but it can also be higher due to promoted cracking of reactants or surface ligands (d). For temperatures within the window a complete monolayer is formed per ALD cycle. The behavior indicated by a dashed line indicates growth limited by surface reconstruction effects, which results in a growth rate below on monolayer per cycle.

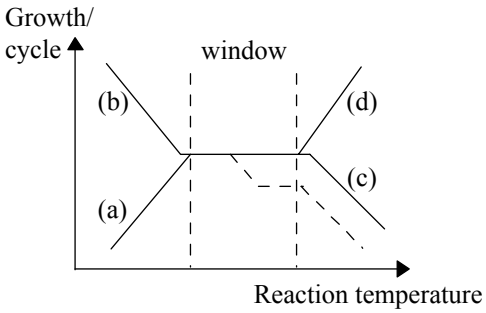

Figure 7: Temperature window of ALD processing, defining the temperature region where the saturation density is one monolayer per ALD cycle.

All process work was done on a F-120 traveling wave reactor, from ASM-Microchemistry Ltd, which is designed for small area substrates, limited to a size of 5×5 cm^2. A traveling wave reactor is based on laminar flow in small volumes, which allows for a fast cycling of the reactant pulses. The reactor chamber is constructed of quartz glass and heated by resistive coils.

5.2 Direct ALD ZnO devices

5.2.1 Background

The most obvious way to avoid the CdS buffer layer is simply to omit it or to replace it with highly resistive ZnO (here referred to as a direct ZnO device). The necessity of an intrinsic layer has been stressed by Olsen *et al.* [35] and direct doped ZnO devices is suggested to suffer from current loss due to Al diffusion into the Cu(In,Ga)Se_2 absorber. In this work the ALD process has been used to develop a direct ZnO device. Some work has been reported on direct ZnO devices with sputtered oxide [19] but with its assumed benefit of being more gentle towards the substrate, the ALD process was proposed as a method for the soft formation of the direct ZnO structure [36-38]. Stolt *et al*. conclude that a substrate temperature of 150 ºC during ALD ZnO deposition is optimal for device performance (η = 11%) but at this temperature the sheet resistivity is too high for module applications. Shimizu *et al*. [38] have determined an efficiency at 13.1% for direct ALD ZnO devices. They use absorbers prepared the two-stage process with selenization/sulfurization in H_2Se and H_2S. In spite of the S rich surface layer, which is assumed to be passivated, the authors emphasize the need for extensive post treatment for this structure in order to reach optimal performance. Today, the best results for the direct ZnO structure is obtained by MOCVD. Olsen *et al.* have

reported efficiencies of 13.95% for direct MOCVD ZnO/Cu(In,Ga)Se_2 devices [39].

5.2.2 The ALD ZnO proess

Doped and intrinsic ALD ZnO was initially evaluated on Mo-coated and bare glass substrates. ZnO films were formed according to reaction (11) from diethylzinc (DEZn) and water vapor as precursors.

$$Zn(C_2H_5)_2(g) + H_2O(g) \rightarrow ZnO(s) + 2C_2H_6(g) \qquad (11)$$

Gaseous source pulsing time and nitrogen purging time were varied and optimal coverage of DEZn was found at 200 ms and ideal N_2 purge at 400 ms. Substrate temperatures were held between 130 °C and 200 °C. The standard ZnO:Al recipe is illustrated in Figure 8. For deposition of doped films a dopant pulse of 200 ms TMAl was added after the DEZn pulse in every 30th cycle.

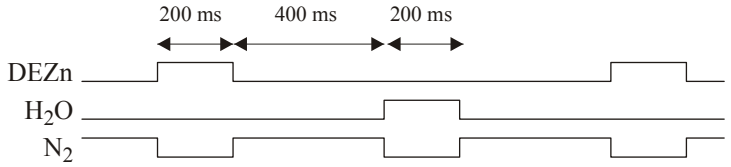

Figure 8: The pulsing schedule used for the ALD ZnO process.

The growth rate on glass substrates was between 1.6-2.2 Å/cycle depending on process temperature. In work by Yamada *et al.* [40] the complete monolayer growth per cycle for (100) oriented films was determined at a growth rate of 2.8 Å/cycle for ALD ZnO synthesized on glass from DEZn and H_2O sources. Possible reasons for the lower growth rate are different orientation, surface reconstruction effects or incomplete saturation of monolayers. The diffractogram in Figure 9 shows a randomly orientated ZnO film deposited by 500 cycles at 150 ºC on Cu(In,Ga)Se_2.

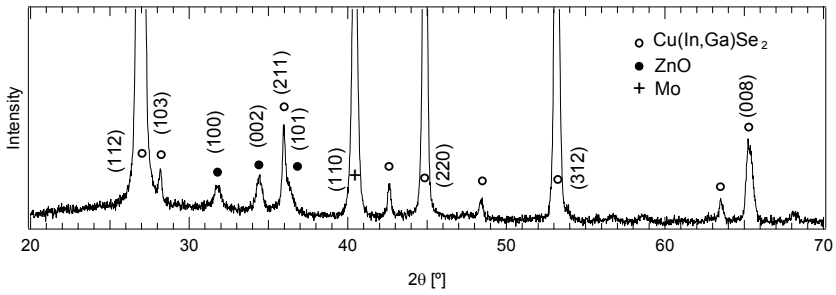

Figure 9: Diffractogram of randomly orientated ALD ZnO grown on Cu(In,Ga)Se_2 by 500 cycles at 150 ºC.

5.2.3 Optoeletrical properties of ALD ZnO films

The Al doped ALD ZnO was investigated at different temperatures and for different dopant concentrations. For a film thickness of 200 nm a maximum transmittance of 93% was determined. Typical resistivity was measured at 2 x 10^{-3} Ωcm with a carrier concentration of $2x10^{20}$ cm^{-3} and mobility between 5-25 cm^2/Vs. Several suggestions for improved conductivity are found in the literature. Yamada *et al*. [40] report resistivity of $7.5x10^{-4}$ Ωcm on ZnO:B grown by UV assisted ALD growth. They observe a mobility of 30 cm^2/Vs for films formed by UV assisted growth. In [41] it is concluded that doping by TMAl should be combined with a DEZn pulse before H_2O is introduced into the reactor for conductivity gain. Moreover, the resistivity of ALD ZnO:Al is known to decrease for higher deposition temperatures [42] and with longer nitrogen purge time.

A haze factor of 12% at λ=500 nm was extracted from transmittance measurements on ALD ZnO:Al deposited at 150 °C, with a thickness of 580 nm, see Figure 10. This value is in the low end of values reported for sputtered ZnO:Al where values as high as 54% have been observed for 1000 nm thick ZnO:Al [43].

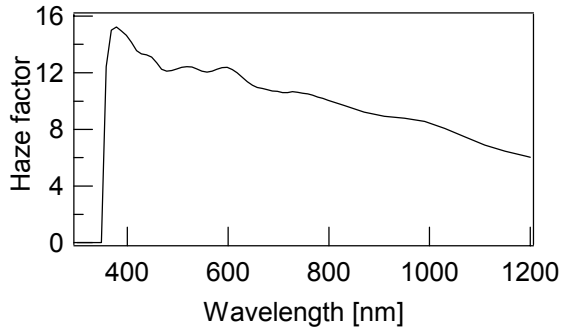

Figure 10: Measured haze factor from ALD ZnO:Al deposited on soda-lime glass. The haze factor increases for shorter wavelength since the texture is more scattering here.

Undoped ALD ZnO was fabricated according to the process in Fig 8. The resistivity for films made with this process was about 10^3 Ωcm. Oxygen vacancies are probably responsible for the rather low resistivity in these films. It was found that the addition of an oxygen pulse after the water pulse in each cycle resulted in an increased resistivity of 10^5 Ωcm.

5.3 Results of direct ZnO devices

Disregarding the low growth rate, it is of some interest to develop an all-ALD window structure, as it could be deposited in an uninterrupted process. Yosfi *et al.* report on solar cell structures with an ALD ZnO/ALD In_2S_3 window resulting in cell efficiencies of 13.5% [42]. Some efforts were made to deposit an all-ALD window within this work. Conductive ALD ZnO:Al was deposited on a 100 nm thick ALD i-ZnO layer deposited on $Cu(In,Ga)Se_2$. Electrically these devices were essentially inactive. The poor performance is not explained by electrical or optical properties of the ALD window layers determined on glass. The likely reason for

the defective devices is instead nucleation failure (see Section 5.7) with formation of an incomplete i-ZnO layer as a result. Instead the effort concerning direct ALD ZnO has focused on replacing the CdS layer and/or the sputtered i-ZnO layer by an ALD i-ZnO layer. Thickness and material for all other layers were chosen similar to that illustrated in Figure 1.

The results from the direct ALD ZnO study are reported in Paper I. The major conclusion is that growth under these conditions is controlled by the nucleation of initial monolayers, rather than being surface limited as predicted by theory [30]. Substrate age and Na content have a negative impact on the growth process. By using freshly prepared or pre-treated absorber surfaces the growth conditions are generally improved and once nucleation is established the growth process continues at the expected rate.

For devices with ALD ZnO buffer and standard sputtered ZnO:Al layers the highest efficiency of 11.7% is reported in Paper I. The devices required post deposition treatments for optimal performance, see Section 5.6. These devices were deposited without a sputtered layer of i-ZnO. The thickness of the ALD i-ZnO layer was optimized with regard to efficiency.

5.4 Alternative ALD buffer materials

Several sulfides, selenides, and oxides prepared by ALD have been investigated for use as Cd-free buffer materials. For a majority of these efficiencies close to or above 10% and in some cases 16% are reported, see Table 2. The devices with efficiencies at about 16% both exhibit high V_{oc} (> 660 mV) but comparably low J_{sc} (~32 mA/cm^2). Today, best result by ALD is achieved with In_2S_3 buffer material. The remarkably thick buffer layer reported for ZnO is deposited on a $Cu(In,Ga)(Se,S)_2$ absorber prepared by selenization followed by sulfurization. Obviously a large number of potential ALD buffer materials remain to be examined.

Table 2: Reported cell efficiencies and thickness for buffer layers deposited by ALD.

Material	*Sources*	*Absorber*	*Efficiency*	*d [nm]*	*Ref.*
ZnO	DEZn, H_2O	$Cu(In,Ga)(Se,S)_2$	13.1%	75	[38]
Zn(O,S)	DEZn, H_2S, H_2O	$Cu(In,Ga)Se_2$	16%		[44]
ZnSe	Zn, Se	$Cu(In,Ga)Se_2$	11.6%	10	[45]
In_2S_3	$In(acac)_3$, H_2S	$Cu(In,Ga)Se_2$	16.4%	30	[46]
TiO_2	TiCl4, H_2O	$CuInSe_2$	0.7%	50	[47]
Ta_2O_5		$CuInSe_2$	5%	1	[47]
Al_2O_3	TMAl, H_2O	$CuInSe_2$	9%	1	[47]

5.5 The ALD In_2S_3 buffer

The In_2S_3 buffer material has been thoroughly investigated and reported by other groups [48,49]. Recently an ALD In_2S_3 device of 16.4% efficiency was reported [46]. Bandgaps between 2.1 and 2.9 eV have been determined for PVD In_2S_3 and

the size of the bandgap is shown to be related to the Na content and grain size of the film [50].

Alternative ALD indium sources for the In_2S_3 process are $InCl_3$ and trimethylindium, but low temperature and simple handling support the use of indium acetylacetonate ($In(CH_3COCHCOCH_3)_3$) abbreviated as $In(acac)_3$. ALD In_2S_3 is grown from solid phase $In(acac)_3$ and H_2S according to reaction (12). The indium source is heated to 130 °C in order to reach a vapor pressure suitable for the ALD reactant flow.

$$3H_2S(g) + 2In(acac)_3(g) \rightarrow In_2S_3(s) + 6acacH(g) \qquad (12)$$

Results from the investigations on ALD In_2S_3 buffer layers are reported in Paper VI. Growth was evaluated on glass and Cu(In,Ga)Se_2 substrates see Section 6.3.2. The influence of process temperature and buffer film thickness on the device parameters was investigated. An observed tendency for increased device performance for temperatures below 140 ºC and above 160 ºC, was found, mainly due to increased V_{oc} and *FF*. Best efficiency for this structure was measured to 12.1% with V_{oc} = 660mV, J_{sc} = 26.9mA/cm^2 and *FF* = 68.4% for a 50 nm thick In_2S_3 buffer. The loss compared to the 16.4% efficient device reported for this structure [46] is due to lower fill factor (78%) and current (34 mA/cm^2). The loss in current is explained by interface recombination, see Section 6.3.3.

5.6 Metastability and light soaking effects

As mentioned in Section 2.3.3 Cd-free devices normally suffer from metastable effects. In Paper I it is observed that V_{oc} and *FF* for direct ALD ZnO devices improve considerably after extensive heat treatment and light soaking. It is suggested that ALD i-ZnO cells require more heat treatment and light soaking but also that these devices can withstand heat better than standard cells with CdS buffer. Metastable effects were observed, however, as part of the gain in performance normally was lost after some time. Light soaking effects due to variation in V_{oc} and *FF* for direct ALD ZnO devices are confirmed and discussed in the work by Platzer *et al.* [51] and Chaisitsak *et al.* [26]. It is reported that different treatments of the Cu(In,Ga)Se_2 surface before ZnO deposition can reduce the metastable effect of the electrical performance. A clearly different behavior is observed in Paper VI for the ALD In_2S_3/Cu(In,Ga)Se_2 devices. Best performance is achieved before air annealing. After annealing devices recover after a certain period of inactivity.

5.7 ALD buffer growth issues on Cu(In,Ga)Se_2

According to the ALD theory, growth is controlled by saturation of surface layers instead of the reactant supply rate, which is the limiting factor for CVD. Critical for the growth is the nucleation phase when initial clusters are formed. Deviations from the ideal growth behavior are observed in Papers I, V and VI. Results show that a conditioned Cu(In,Ga)Se_2 surface in general is more likely to promote nucleation, independent of temperature within the process window. This is clearly demonstrated when part of a Cu(In,Ga)Se_2 sample was water treated prior to the ALD process. In Figure 11 a partly water dipped Cu(In,Ga)Se_2 sample is shown after ALD ZnO deposition. The dark areas represent the water-dipped surfaces

were ZnO growth was normal while the untreated light diagonal stripe showed no nucleation. Film formation is unambiguously correlated to the water treatment. The flow direction of reactants is downwards in the picture. As the source gas passes the surface nucleation begins, is occasionally interrupted, and then continues. It is concluded that the ideal nucleation process of a neighboring area has no effect in an area where the conditions do not meet the required properties for growth. A positive effect on nucleation is also accomplished by conditioning the sample in DEZn. Two possible reasons for poor growth are hence considered: (a) an easily soluble compound residing at the $Cu(In,Ga)Se_2$ surface, which is counteracting the nucleation or (b), the lack of necessary radicals at the surface e.g. OH^-. A combination of these obstacles has been suggested to be responsible for the observed difficulties of nucleation. Pretreatment in H_2 at 150 ºC was also evaluated and found to have no impact on the formation of monolayers. A series of $Cu(In,Ga)Se_2$ samples was run through the above treatments and analyzed to separate the effects of the water treatment versus DEZn conditioning. Results from these treatments are discussed in Sections 5.7.3 and 5.7.4.

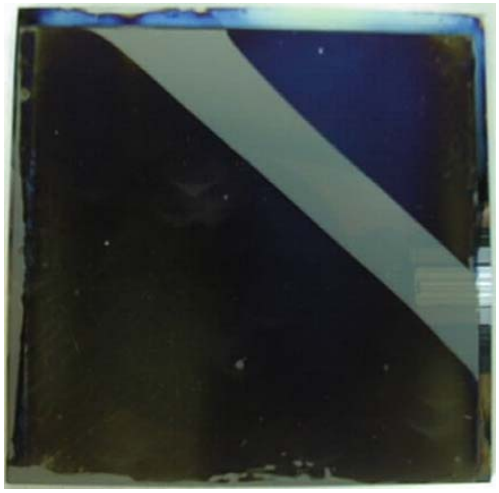

Figure 11: ALD ZnO grown on partly pretreated $Cu(In,Ga)Se_2$. The sample was diagonally dipped in de-ionized water for 10 s from upper right and lower left corners. The dark areas exhibited normal ALD growth.

5.7.1 Substrate aging

After deposition of the chalcopyrite absorber the ageing process begins immediately when the sample is subjected to air. This transformation is impeded by storage in vacuum or in an inert environment. As a consequence of air exposure, oxidized states of In and Se have been identified by Kessler *et al.* [21]. Oxidation is enhanced by the presence of Na and the formation of Na-O-C compounds has been suggested by Ruckh *et al.* [52]. Detailed models have been reported which explain how oxidation, by air exposure or O_2 annealing, primarily occurs at surface defect sites forming In-O bonds catalyzed by Na [53,54]. A more complete picture of the oxidation process of $Cu(In,Ga)Se_2$ in air is given in work by Scheer [55].

In order to investigate the nucleation on unexposed $Cu(In,Ga)Se_2$ surfaces, experiments with a Se cap layer have been performed. The deposition of the absorber was finalized by the deposition of a thin Se layer to protect the surface of the absorber from air exposure. Inside the ALD reactor the Se cap layer was removed by annealing at 220 °C before the ALD process was started. No nucleation and growth disturbances were observed at the unexposed surface and a homogeneous ZnO film was deposited.

5.7.2 Pretreatment with water

The removal of sodium from an air exposed $Cu(In,Ga)Se_2$ surface by water treatment and the reappearance after heat treatment has been reported by Bodegård *et al.* [56]. It has been suggested that sodium is present in the form of Na_2SeO_4 [57]. Before and after water treatment of similar baseline material, the presence and removal of Na_2CO_3 is pointed out by Kylner [58]. According to Kessler *et al.* [21], the presence of native indium and selenium oxides is not changed by a water dip. Gallium oxide is insoluble in water. Hence most metal oxides are ruled out as explanation for the observed change in ALD ZnO nucleation. Earlier experiments on our $Cu(In,Ga)Se_2$ material have also shown that Na appears after the water treated substrate was heated in vacuum for 1 hour at 300 °C and irreversibly disappears upon vacuum heat treatment for 1 hour at 550 °C [59]. In Paper V the surfaces of aged, water dipped aged, fresh, and water dipped fresh $Cu(In,Ga)Se_2$ absorbers are compared by XPS. This study gives information about the surface of the samples, which are normally loaded into the ALD reactor and the surface after the temperature ramp up. It is the heated surface that is subjected to the ALD process. It is concluded that ALD growth can be initiated although the $Cu(In,Ga)Se_2$ surface contains oxides when loaded into the reactor. The obvious and diverse impact of the surface chemistry motivates a thorough investigation of how the water treatment followed by the temperature ramp of the ALD process influences the growth.

5.7.3 Simulation of an ALD process with water treatment

The ALD process was simulated and recorded from a $Cu(In,Ga)Se_2$ sample by analyzing the untreated surface (i), the surface after 10 s water dip (ii), and after water dip and vacuum annealing at 150 °C (iii), which is assumed to correspond to the surface when the cycling of ALD reactants is started. Photoelectron spectra reveal the effect of water treatment on Na, O and C. In Figure 12 the Na1s, O1s and C1s peaks before and after water dip and after heat treatment are shown. Clearly as nucleation is supported by (iii) the presence of an arbitrary Na compound alone does not explain the absence of nucleation as opposed to the Na-C compound, which is removed by water.

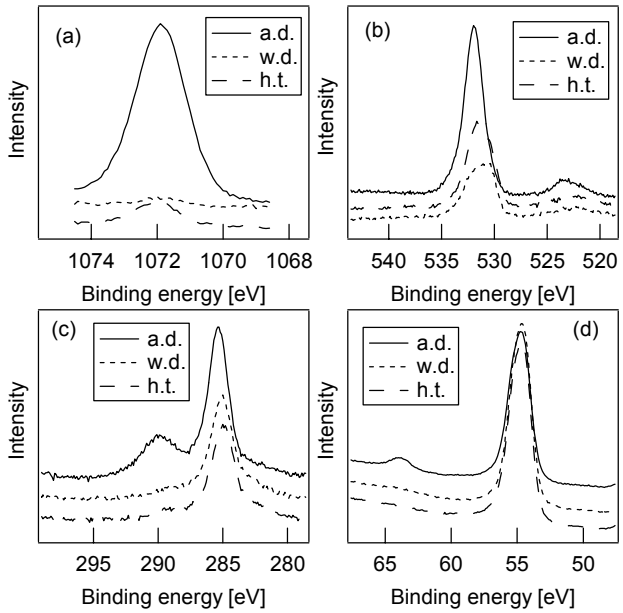

Figure 12: Na1s (a),O1s (b), C1s (c), and Se3d (d) peaks collected during a simulated ALD process in three steps: (i) as deposited (a.d.), (ii) water dipped (w.d.) and (iii) heat treated (h.t.) Cu(In,Ga)Se_2. All spectra collected with non-monochromated Mg K_α and pass energy of 20 eV.

The Auger parameter for Na was determined to $\alpha' = 2061.4$ eV and together with the removed and reduced C-O bonds in the C1s and O1s peaks respectively, see Figure 13 (a) and (b), it is suggested that Na_2CO_3 ($\alpha' = 2061.3$ eV [60]) is removed at (ii). Binding energies are within 0.2 eV of values reported by Kylner and by Lyahovitskaya *et al.* [58,61]. It is clear from the Se3d structure that the Na compound cannot be Na_2SeO_4 mentioned earlier [62].

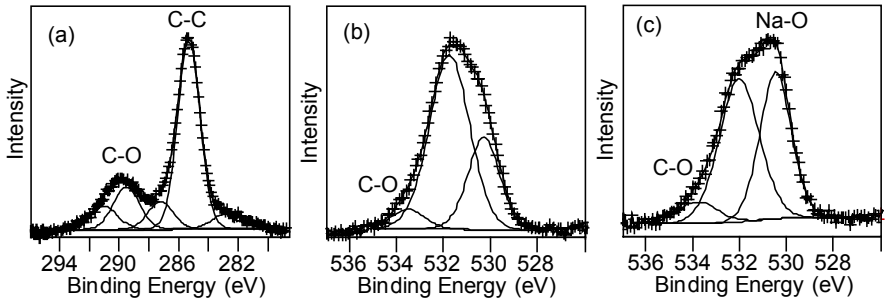

Figure 13: Deconvolution of the C1s peak (a) from the untreated Cu(In,Ga)Se_2 and the O1s peak after water dip (b) and heat treatment at 150 ºC (c). All spectra collected with non-monochromatic Mg K_α and pass energy of 20 eV.

After vacuum annealing (iii), Na has diffused to the surface from the bulk, The Auger parameter determined at $\alpha' = 2062.3$ eV indicates that Na_2O ($\alpha' = 2062.3$ eV [60]) is formed which is also supported by the increased Na-O component at 530.2 eV in Figure 13 (c). The chemical state of the observed Na at the annealed surface is of certain interest since this surface (iii) allows ideal ALD growth.

Ideal ZnO growth is observed on $Cu(In,Ga)Se_2$ deposited on barrier substrate and on alumina substrates (absolutely sodium free). Both of the Na-free substrates also differ from the baseline by increased surface roughness, which might act beneficially on monolayer formation.

5.7.4 Analysis of DEZn treatment

Consequences of the DEZn treatment were analyzed by XPS depth profiling. Two questions were addressed here: the change of chemical state of the surface as a result of the process and the in-diffusion of Zn into the absorber. A $Cu(In,Ga)Se_2$ film was heat treatment in an DEZn atmosphere at 150 °C for 10 minutes. From depth profiling it was concluded that Zn is present at and below the surface. Profiling was performed by Ar sputtering for 75 minutes, at 2kV discharge voltage, 600 V acceleration voltage and 5 mA current.

As a result of DEZn treatment at 180-200 °C the diffusion of Zn in $Cu(In,Ga)Se_2$ has been observed as reported by Sugiyama *et al.* [63]. The authors suggest the formation of a buried homo-junction that reduces metastable effects and the light soaking requirements. This was not observed on pretreated devices in this study.

6 *In vacuo* studies of ALD film growth

6.1 Background

Much effort has been put into a valid *in situ* analysis of the surface limited reactions occurring during the ALD growth cycle. A brief discussion will be made here on the methods used for *in situ* analysis. By use of quartz crystal microbalance (QCM) the stabilized mass differences are measured after each ALD pulse [64,65]. The mass increase is $\Delta m_0=|\Delta m_1-\Delta m_2|$ during one ALD cycle, where Δm_1 is due to the absorption in the first pulse and Δm_2 due to reaction in the second pulse. The molecular weight ratio $\Delta m_0/\Delta m_1$ is then used to confirm the reaction that has occurred. Rosental *et al.* has reported on *in situ* characterization by p-polarized reflectance spectroscopy (PRS). Incremental changes in reflectance of the substrate surface is studied as ALD monolayers are grown [66].

Ritala *et al.* have employed residual gas analysis for *in situ* characterization of the ALD process [67]. The method gives information on the chemical reactions but interpretation of data is fairly complicated. A similar method was also evaluated in our ALD reactor. It was concluded that the reactant ligands were modified by the QMS analysis. Welzenis *et al*. have reported on *in vacuo* low energy ion scattering for investigation of ALD growth [68].

QCM and PRS are suited for *in situ* analysis mainly when normal nucleation of monolayers exists. RGA provides chemical information regardless of the growth state. Since the process cycle alternates between two phases of the reaction area it is of special interest to gain knowledge about and to resolve the chemical state of the substrate surface within a process loop. This work contributes by adding detailed *in vacuo* XPS analysis of the ALD growth on various substrates. The obvious motivation lies within the nucleation and growth related issues reported in Paper I. In addition the setup provides the opportunity of detailed monitoring of the valence band alignment during the deposition of monolayers to a semiconductor surface.

In situ means “in its original place” and refers to that a sample is analyzed in its proper position during process. In this thesis the term *in vacuo* is used since the sample is actually moved between the events of process and analysis but kept under vacuum all the time.

6.2 Connecting the ALD and XPS system

In Paper IV the coupled XPS-ALD system is described and evaluated. Due to the low vacuum regime in the ALD reactor ($>2\times10^{-3}$ mbar) the sample under investigation has to be transferred for analysis into the chamber of the coupled XPS/UPS system. The two systems are connected through a differentially pumped transfer stage and a gate valve as illustrated in Figure 14. Sample handling is performed by a sample rod for transport between the chambers. In this experimental setup smaller substrates (8×20 mm^2), limited by the diameter of the sample rod, are used. The sample is attached to the rod during the entire experiment. Consequently the gate valve must be kept in open position while the sample is located in the ALD reactor. Differential pumping of the connection stage ensures a pressure in the low range of 10^{-8} mbar in the UHV chamber while the

gate valve is open. With the rod in the extracted position a gate is sealed between the volumes, which allows for a background pressure of 10^{-10} mbar during analysis work. This high vacuum is necessary for He II operation of the He-lamp.

The *in vacuo* UPS analysis offers the possibility to investigate the energetical offset between the valence band in ALD thin films and semiconductor substrates. From He I and He II emission lines, electrons can be excited with energies of 21.21 eV and 40.8 eV, respectively. An uncertainty induced by using another excitation source is the possible difference in geometry of the analyzed area when illuminated by the He lamp or the X-ray tube. However, the analyzed area is mainly determined by the geometry of the input lens of the analyzer.

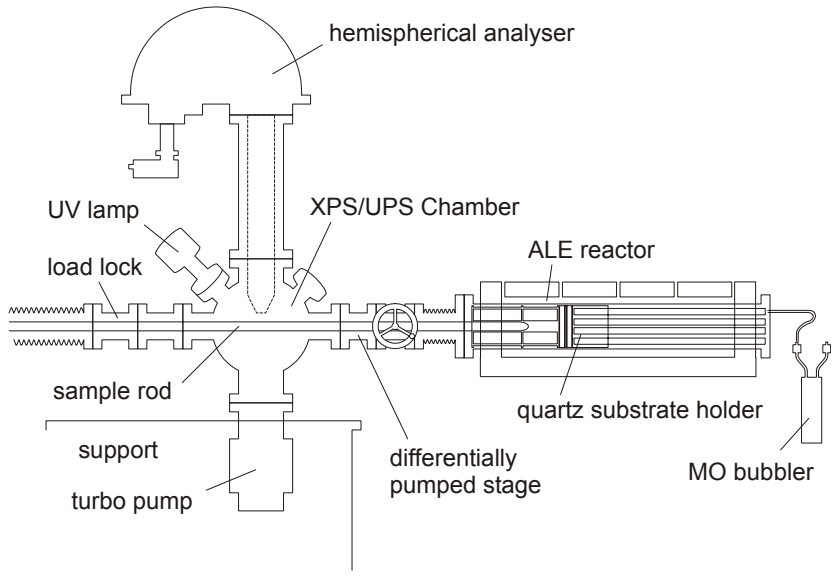

Figure 14: Schematic drawing of the Leybold XPS instrument connected to the ALD reactor for in vacuo analysis.

Thorough modifications of the reactor interior and the deposition zone were necessary to facilitate the substrate transfer. Changes were made to the quartz parts and the stainless steel support arms. The impact of these modifications on the conditions for ALD growth regarding reactant flow, prolonged pulsing time and temperature control in the rebuilt reactor is treated in Paper IV. It can be concluded that ALD growth is maintained in spite of these extensive changes. The conditions necessary to consider the analysis to be a valid description of the standard process in the ALD reactor were investigated. Four criteria for retention of the ALD process were identified:

- Differences between the standard ALD and the modified reactor with regard to temperature and time during the period between sequencing pulses do not affect the process.
- Reactants, which are absorbed at the substrate surface, do not desorb or undergo change in chemical state when the surrounding atmosphere is

changed into ultrahigh vacuum or when the surface is exposed to X-ray radiation.
- Flow conditions are not drastically changed as a consequence of the modifications, which have been made to the substrate holder, concerning sample position and process volume, pressure, temperature etc.
- Pulse duration can be increased as compared to a standard ALD recipe.

Problems inherent to the design modification were observed and are reported in Paper IV. In addition, fluorine and carbon originating from organic sealing materials in the lock were contaminating the substrate at high substrate temperature ~400 ºC. This deviation from the standard process was not discussed or tested in Paper IV. The increase of C observed in Paper IV was assumed to be related to the incomplete removal of ethyl groups from the DEZn precursor. Suggested improvements are to replace the C-containing sealings or to use a modified sample rod with selective cooling of the section, which is positioned within the lock. The second criterion is of importance mainly when submonolayer formation is target for the analysis. In the ideal case of ZnO deposition on Si wafers, chemical shifts related to the absorption of reactant molecules were traceable even though the pressure surrounding the sample was lowered by 7 orders of magnitude (see Section 6.3.1). For ALD film growth on $Cu(In,Ga)Se_2$ substrates however, the film increment of interest varies between single monolayers and tens of cycles depending on the experimental topic. Inhomogeneous film growth was observed on the quartz parts of the reaction chamber as a consequence of the insertion of the sample rod. This indicates that the third criterion is not completely fulfilled. In Figure 15 it is seen that the In_2S_3 process at 160 °C with 1000 cycles leaves a poorly covered region just below the hole. The area above the hole exhibits uniform growth and hence substrates facing upwards most likely experience standard growth conditions.

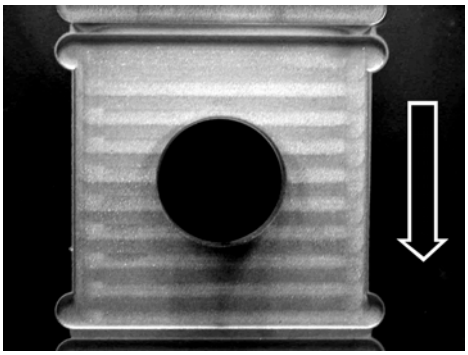

Figure 15: The quartz substrate holder showing growth disturbance below the hole due to sample rod insertion. The arrow indicates flow direction of reactant gases.

The two-sided sample rod, later extended to four sample holding sides, allows for different samples to be processed and analyzed under identical conditions. Hence it can be used in experiments where various substrate properties must be distinguished, for example substrates with and without sodium. The rod is

equipped with a thermocouple and heating/cooling capabilities used to cool the sample after processing before it is brought into the XPS chamber.

6.3 *In vacuo* PES study of ALD ZnO and In_2S_3 growth

6.3.1 Reference study

Detailed *in vacuo* analysis was conducted for the ZnO process using glass, sapphire and crystalline silicon as substrates. Silicon substrates were superior for analysis since substrate emissions did not overlap. A proof of concept was achieved as alternating intensity ratio between components of the O1s peak after DEZn and water reactant pulsing was observed. Two chemical states of the processed surface could be demonstrated qualitatively, see Figure 16 (a). Growth is expected to begin easily on the controlled surface and nucleation was obviously initiated during the first cycle. In Paper IV is reported briefly on the ZnO formation on the Si substrate.

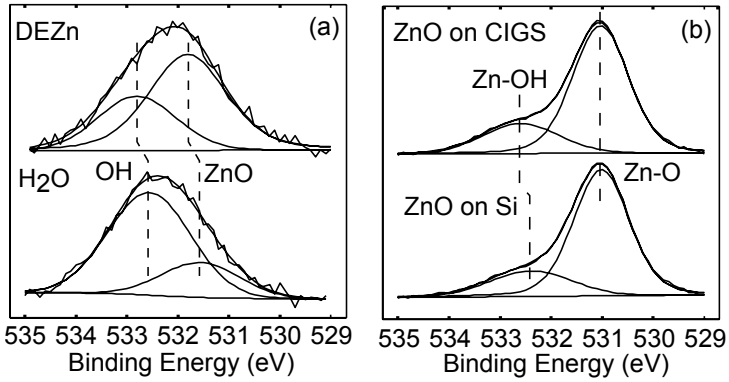

Figure 16: Alternating intensities of Zn-O and H-O bonds during the initial ALD cycle on a Si substrate (a). The O1s peak from thick ZnO on Si and Cu(In,Ga)Se_2 substrates (b).

The initial DEZn pulse results in a Zn2p signal and an additional O-Zn component contributing to the O1s peak. After the subsequent H_2O pulse the relation between the intensities of the O-H and the O-Zn components of the O1s peak is reversed. Additional pulses render the same alternating behavior but emissions from the completed ZnO layers beneath the top layer also contribute to the spectra. For thick films with more than 100 cycles the O1s peak clearly contains two components, separated by 1.4 eV, see Figure 16 (b). The dominating component at lower BE (~531 eV) corresponds to the bulk ZnO while the smaller component at about 532.4 eV is suggested to represent a Zn-OH phase. This is observed for film deposition on Si as well as Cu(In,Ga)Se_2 substrates (see Paper V).

6.3.2 ALD growth on Cu(In,Ga)Se_2

In Paper V it is reported on the results from the *in vacuo* study of ZnO growth on Cu(In,Ga)Se_2. The progress of ZnO formation on water treated Cu(In,Ga)Se_2 surfaces is similar to the observations from the reference study on Si substrate. The

nucleation occurs during the first cycle and growth continues as expected during subsequent cycles. However, a distinct separation of the different oxides, that were present during the initial cycles in the reference study, was not observed on $Cu(In,Ga)Se_2$. The reason for this is the additional native oxides present at the $Cu(In,Ga)Se_2$ surface. The influence of the order of reactants was investigated on $Cu(In,Ga)Se_2$. Processes that started with a H_2O pulse instead of a DEZn pulse were identical except for a delay of one pulse and it is concluded that the growth process begins at the DEZn pulse.

On fresh but untreated $Cu(In,Ga)Se_2$ substrates a growth delay occurs, during which the chemical state of the surface is changed and only small amounts of Zn are observed. In Paper V the disappearance of the C1s peak at 290 eV indicates that the originally present Na_2CO_3 is removed during this time. It is suggested that the effect of the initial DEZn pulses is to be etching Na_2CO_3 away until bare $Cu(In,Ga)Se_2$ is reached after which ZnO growth begins. The *in vacuo* monitoring of a fresh $Cu(In,Ga)Se_2$ surface during the first seven cycles of the ALD ZnO process is shown in Figure 17, illustrating the Cu2p, In3d, Se3d, O1s, Zn2p and C1s peaks. This process started with a H_2O pulse. Spectra were acquired after single reactant pulses, each of 5 seconds duration. During these cycles, ZnO growth was not started and a different Zn compound was initially formed. Instead the O1s peak decreases due to reduction of surface oxides. In the C1s spectra removal of the C-O bond is seen. After some delay, the formation of ZnO layers begins. In the Zn2p and O1s spectra acquired after 107 completed cycles the presence of ZnO was confirmed (not shown here).

The In_2S_3 growth on aged/fresh and water treated surfaces was also compared. It was apparent how much more effective the nucleation of the reactants used for In_2S_3 occurs and the growth proceeds. In Paper VI the film is identified as In_2S_3 already after the initial 20 cycles are completed. No pre-treatment was done to the $Cu(In,Ga)Se_2$ absorber and yet all buffers exhibited highly uniform films, free from voids. It is likely that Na_2CO_3 is located at the surface of the aged substrates. A possible effect is that this compound is embedded at the $In_2S_3/Cu(In,Ga)Se_2$ interface. Still, the growth rate is improved by surface conditioning with water.

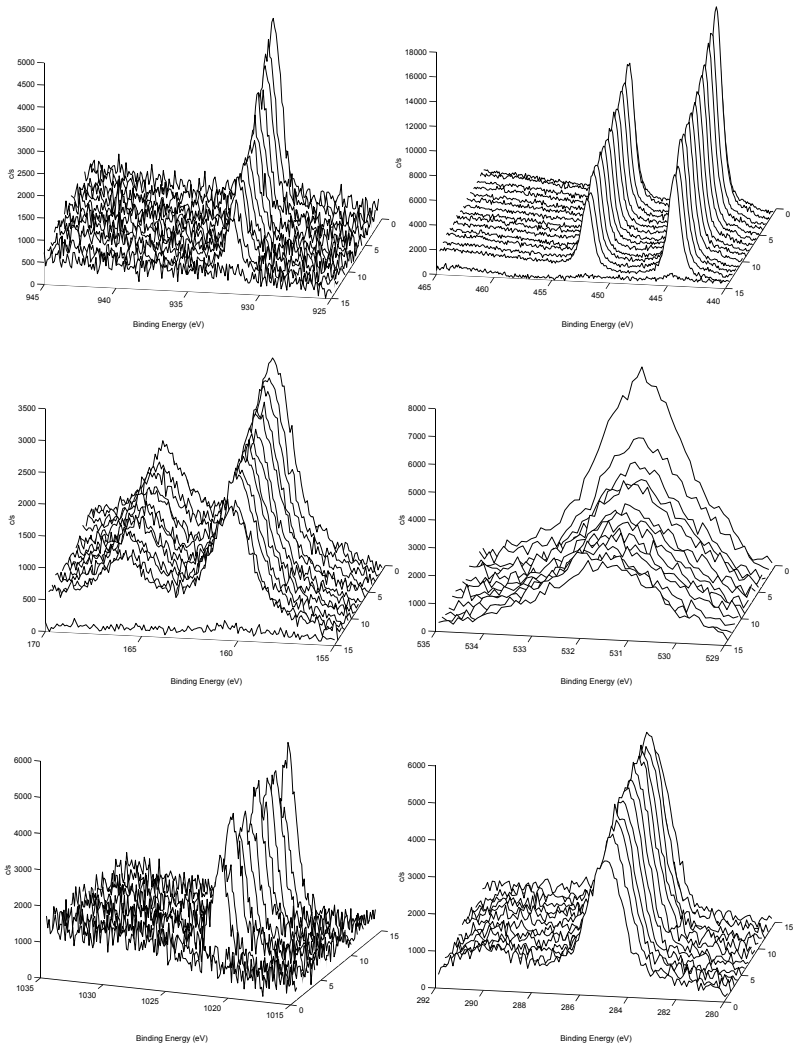

Figure 17: Decreasing Cu2p, In3d, Se3d, O1s peaks (spectra in reversed order), and increasing Zn2p and C1s peaks (spectra in chronological order). Initial spectra show untreated fresh Cu(In,Ga)Se_2 and subsequent spectra after alternating H_2O and DEZn pulses with 5s duration. The last step includes 100 cycles (omitted for Zn2p).

6.3.3 Band alignments

Several band alignment studies have been made in the combined XPS-ALD system. In Paper V $\Delta E_C = -0.2 \pm 0.2$ eV is reported for the direct ALD ZnO/Cu(In,Ga)Se_2 interface. The low values of V_{oc} reported for direct ZnO devices prior to air annealing in Paper I can be explained by the negative offset, which is expected to result in an increased interface recombination compared to the CdS

reference. In work by Platzer *et al.* the direct ZnO/Cu(In,Ga)Se_2 and ZnO/$CuInSe_2$ interfaces are compared and the ΔE_C for the latter found to be slightly positive (ΔE_C = +0.1 ±0.2 eV) [51]. The authors discuss the connection between the higher voltages observed for the ZnO/$CuInSe_2$ structure and the positive ΔE_C.

In Paper VI an investigation of the ALD In_2S_3/Cu(In,Ga)Se_2 interface is reported. In this study the influence of Na on ΔE_C is analyzed. This is motivated by the fact that E_g for In_2S_3 is reported to vary strongly (2.1 - 2.9 eV) if small amounts (0 - 6%) of Na is present in the film [50]. In Paper VI it was found that only limited amounts of Na, if any, diffuses into the In_2S_3 film. E_g was determined at 2.1 eV for films deposited on glass independent of the Na content of the glass. This value is smaller than what is generally reported for ALD In_2S_3 films. The difference is explained by the method for E_g determination. Values for ΔE_V were observed to be related to the Na content and was achieved at -1.2 ±0.2 eV for the junction with Na present and at -1.4 ±0.2 eV with Na free Cu(In,Ga)Se_2. The reason for this difference is not known but one likely interpretation is contaminations at the surface of the Na containing Cu(In,Ga)Se_2 layer (see section 5.7.1). With a typical E_g for the Cu(In,Ga)Se_2 film of 1.1 eV this will give ΔE_C = -0.2 ±0.2 eV with Na present and ΔE_C = -0.4 ±0.2 eV on Na free absorbers. For device application only the Na containing material is of interest since Na to a large extent determines the quality of the Cu(In,Ga)Se_2 layer. The negative offset found in this study is in contradiction with the high efficiencies reported for Cu(In,Ga)Se_2 devices with ALD In_2S_3 buffers and the high V_{oc} observed in Paper VI. At the temperature used for ΔE_C determination, however, the device voltage is lower. The low J_{sc} and *FF* determined for In_2S_3 devices in Paper VI rather indicate a positive offset if any. The low current is more likely explained by recombination at the In_2S_3/Cu(In,Ga)Se_2 interface.

7 Sulfurization of $CuIn_xGa_{1-x}Se_2$ absorber layers

7.1 Motivation for sulfurization

This part of the work describes two different approaches to modify the chalcopyrite absorbers by post-deposition treatment in an H_2S atmosphere: sulfur grading at high temperature (> 400 ºC) and surface conditioning at low temperature (< 400 ºC). The background and motivation for each method is briefly discussed before the main results are presented.

7.2 Decreased losses by sulfur grading

At open circuit conditions a substantial part of the recombination is expected to occur in the SCR as discussed in Section 2.2.2. A widening of E_g will result in a reduced recombination rate, R~np. An advantage of the $CuInSe_2$ material is that E_g easily can be changed. An increased E_g can be accomplished by introducing for example Ga, or S into the material. By introducing S mainly the energy position of the valence band will be lowered while an introduction of Ga will result in a raised conduction band level [69].

If uniformly added, E_g will increase through the entire absorber depth, resulting in an increase of V_{oc} but a decreased light absorption and smaller J_{sc}. With a tailored composition profile the bandgap can be selectively increased at the front and/or back of the absorber layer. An optimized profile will lead to an enhanced absorption of the incident light as compared to a homogeneously wider bandgap, while still maintaining a higher V_{oc}. When increasing the conduction band in the front (i.e. increased Ga concentration) a cliff for electrons might appear in the conduction band ($\Delta E_C < 0$), which can increase the interface recombination. No experimental results has proven a beneficial effect of increasing Ga/(In+Ga) at the front of the absorber layer [70]. When lowering the valence band instead (i.e. increased S concentration) there is no risk of forming a cliff for electrons in the conduction band, see Figure 18. A lowered conduction band will reduce the hole concentration and result in decreased recombination. This is confirmed experimentally by Walter *et al.* [71]. They have found that the hole concentration decreases exponentially with the S/(Se+S) ratio if no Ga is present. With Ga present this effect appears when S/(Se+S) > 0.3.

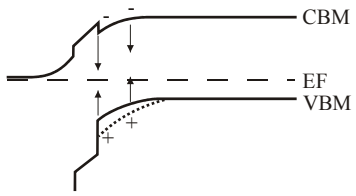

Figure 18: Qualitative band diagram showing a $Cu(In,Ga)Se_2$ layer (solid line) and the lowered valence band (dotted line) as a result of sulfur incorporation in the surface layer.

A beneficial effect from grading with S instead of Ga is anticipated in aspects of energy band alignment for the direct ZnO device. For the formation of a heterojunction between ZnO and $Cu(In,Ga)Se_2$, a sulfurized surface with low Ga content is preferred compared to an unsulfurized Ga containing surface, since the value of ΔE_C will be in favor for the sulfurized material.

7.2.1 Methods for sulfur incorporation

For reasons of optimization, the complex absorbers described here normally contain not just one homogeneous phase but contain concentration profiles. Tuttle *et al.* conclude that a critical issue is to find a method that is suited for a particular absorber structure [72]. The $Cu(In,Ga)Se_2$ absorbers used in this work are prepared by coevaporation. This method can be extended to deposition of the pentenary system. Shafarman *et al*. have reported that coevaporated $Cu(In,Ga)(Se,S)_2$ absorbers tend to grow S/(Se+S)-poor [73]. Kötschau *et al*. find that the best pentenary absorbers are obtained from an In-rich growth mode [74].

$Cu(In,Ga)Se_2$ can be prepared by a two-stage process with selenization of metal precursors [75] or rapid thermal processing of stacked elemental layers [76]. In and Cu-Ga precursor layers are sputtered onto Mo coated glass substrate and selenized in an H_2Se atmosphere at elevated temperatures. This method is also used to prepare $Cu(In,Ga)S_2$ films where selenization is replaced by sulfurization in H_2S, or with both gases combined to fabricate $Cu(In,Ga)(Se,S)_2$ absorbers with a graded composition and an S-rich surface [77].

Incorporation of S has also been shown by post deposition annealing of $Cu(In,Ga)Se_2$ absorbers in an S rich environment. Nakada *et al.* has reported on sulfurization by annealing of $Cu(In,Ga)Se_2$ absorbers in H_2S [78]. They used $Cu(In,Ga)Se_2$ films prepared by a multistage process with increasing Ga concentration towards the back contact. The device efficiency was increased from 11% to 14.3% as a result of the H_2S process. Annealing of $Cu(In,Ga)Se_2$ films in elemental S vapor is reported by Ohashi *et al*. [79] to give an increase in efficiency from 15.8 to 16.2%.

Engelmann *et al*. has suggested a model for the reaction/diffusion process that occurs during sulfurization of $CuInSe_2$ films. They suggest a rapid exchange of Se in the surface for S in the H_2S according to Equation 13. An S rich phase is formed at the surface which acts as a sulfur diffusion source. This phase slowly intermixes with the absorber material and forms a solid solution with the $CuInSe_2$ in the bulk.

$$2H_2S(v) + CuInSe_2(s) \leftrightarrow 2H_2Se(v) + CuInS_2(s) \qquad (13)$$

7.2.2 Results from bandgap grading experiments

The sulfurization experiments were carried out in an RTP reactor from Centrotherm. Rapid thermal processing is widely used in microelectronics industry. The process allows for a temperature ramp-up rate of several hundred degrees centigrade per minute. For the $Cu(In,Ga)Se_2$ application RTP is an interesting approach since the glass substrate tends to bend when heated. By the use of RTP the absorber can be heated for a short time and deformation of the glass substrate can be avoided.

The effect of the sulfur treatment was evaluated by GI-XRD (Paper II), TEM (Paper III), SIMS (Paper VII) and cross sectional SEM. From diffractograms, S containing phases were identified in all films. In the $CuGaSe_2$ film a separate $CuGaS_2$ phase was formed after sulfurization (Figure 19 (a)). A similar separation into $Cu(In,Ga)Se_2$ and $Cu(In,Ga)S_2$ phases was observed for the quarternary films. Diffractograms of sulfurized $CuInSe_2$ films instead show a mix of selenide and sulfide phases with an increasing S/(Se+S) ratio towards the front (Figure 19 (b)). This film structure is qualitatively in agreement with the model by Engelmann. In compositional profiles by SIMS, S is present with a gradient throughout the entire layer for all films. S diffusion is, however, strongest in the $CuInSe_2$ film. The explanation for the somewhat different depth profiles, when comparing SIMS and XRD, is that S diffuse through grain boundaries and is detected by SIMS even though it is not incorporated in a grain.

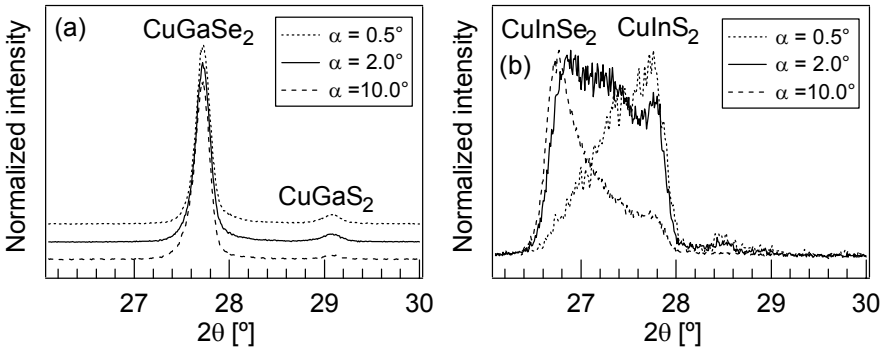

Figure 19: Diffractograms illustrating normalized (112) peaks of $CuInSe_2$ (a) and $CuGaSe_2$ (b) after sulfurization at 525 ºC for 50 minutes as a function of different incidence angles.

From the process at high temperature reported in Paper II and VII it is concluded that post deposition incorporation of S in $Cu(In,Ga)Se_2$ will generate working photovoltaic devices only in absorbers with a Ga-free surface, i.e. $CuIn(Se,S)_2$. The phase-separated film formed in the presence of Ga, probably contain band discontinuities inside the absorber layer. The effect of such steps is not known but increased recombination losses due to the formation of an additional interface are expected. Cell devices made from sulfurized $Cu(In,Ga)Se_2$ were poor. Devices were made with baseline window on $Cu(In,Ga)Se_2$ layers sulfurized at 400, 450, and 475 ºC. Increased voltage was observed only at the highest temperature. This device had very low current. Post deposition sulfurization of coevaporated $Cu(In,Ga)Se_2$ is affected negatively by the surface presence of Ga. The successful results from sulfurization of $Cu(In,Ga)Se_2$ films reported in [78] is likely due to low surface concentration of Ga which is observed for films fabricated by selenization [80].

In Paper VII a strong correlation of Na and S concentration profiles in sulfurized absorbers was observed and the formation of a Na-S compound is suggested which could occur readily at the surface and in the grain boundaries. This compound was identified by GI-XRD and TEM-EDS as $NaInS_2$ in

$CuIn(Se,S)_2$ films but only indicated by GI-XRD as Na_2SO_4 or Na_2SeO_4 in $CuGa(Se,S)_2$ films.

7.3 Surface conditioning in H_2S

While sulfurization with the intention of bandgap widening can be described as an intense method at high temperature where bulk properties of the $Cu(In,Ga)Se_2$ film are modified, surface conditioning by H_2S should be viewed as a soft treatment aiming at modifying properties of the surface only. The ALD buffer/$Cu(In,Ga)Se_2$ devices generally suffer from metastable behavior and require extensive air annealing and light soaking for optimal performance. These artifacts are believed to be related to poor buffer/absorber interface quality. It has been reported that the surface of $Cu(In,Ga)Se_2$ absorbers can be passivated by post-deposition sulfurization [78]. A design with direct ALD ZnO deposited on H_2S conditioned $Cu(In,Ga)Se_2$ absorber is motivated by the anticipated reduction of interface recombination as a result of passivation.

7.3.1 Results from surface conditioned $Cu(In,Ga)Se_2$

$Cu(In,Ga)Se_2$ films treated by the low temperature process were provided with direct ALD ZnO buffer without air exposure of the H_2S-conditioned surface. The electrical performance of these devices was evaluated and compared to unsulfurized CdS/$Cu(In,Ga)Se_2$ and ALD ZnO/$Cu(In,Ga)Se_2$ device structures. Best direct ZnO performance was achieved for a sulfurization process at 120 ºC for 120 minutes. For the H_2S conditioned surface a current gain of 1 mA/cm^2 was determined compared to the device made on untreated $Cu(In,Ga)Se_2$. From the QE plot in Figure 20 it is seen that direct ZnO devices gain from less absorption in the blue wavelength region compared to the CdS/$Cu(In,Ga)Se_2$ cell and that the direct ZnO devices improve by the surface conditioning H_2S process. One possible explanation for this improvement is the passivation of surface states of the $Cu(In,Ga)Se_2$ layer with reduced interface recombination as a result.

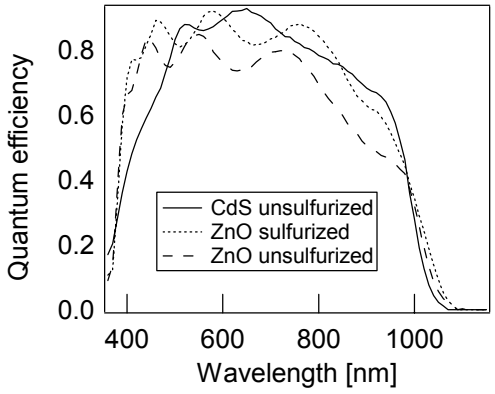

Figure 20: QE plots showing the enhanced spectral response for the direct ZnO device by absorber surface conditioning with H_2S at 120 ºC in 2 hours.

From a valence band study of the H_2S conditioned surface it was concluded that the investigated sulfurization temperatures were too low for S incorporation and the position of the valence band remained unchanged. Thus it is suggested that the beneficial effect of this process is solely related to passivation of the $Cu(In,Ga)Se_2$ surface.

8 Concluding remarks

From the work on ALD buffers for $Cu(In,Ga)Se_2$ devices and modifications of the absorber surface the following conclusion are made:

- Today Cd and the CBD process can be substituted, but yet at the price of lower efficiency and stability. Surfaces and interfaces are important for processing as well as for device performance of the cells. In an industrial context, an additional step of surface pretreatment will reduce throughput and thereby increase the production cost. Moreover, surface conditioning by wet chemistry is unfavorable in an inline vacuum production.
- In an all-vacuum process chain the atomic layer deposition process can be utilized for buffer fabrication probably without any conditioning steps. While an all-vacuum inline process is not yet developed, theoretical work is needed to identify the conditions of the $Cu(In,Ga)Se_2$ surface necessary for the ALD precursors to nucleate. One such method frequently used for characterization of precursors is *ab initio* calculations.
- The beneficial effect of sodium on absorber formation is well known. But Na appearing at the surface and in grain boundaries can have detrimental effects on the device in subsequent process steps such as inhibiting nucleation in ALD ZnO growth. Na interdiffusion into the window has been observed but the effect on device operation is not easily distinguished from effects on the absorber when working with Na-free substrates.
- Surface conditioning has proved to be successful for process and device improvements. Surface conditioning with water or DEZn has primarily an impact on the process while conditioning with H_2S acts beneficially on the electronic behavior. Further investigations are suggested to resolve the mechanisms responsible for the observed metastable behavior and its correlation with different conditioning methods.

This work brings a proof of concept for *in vacuo* monitoring of the ALD process. The inherent flexibility of the ALD method allows for an increased process control. In a developed system with *in situ* controlled parameters the ALD recipe (pulsing time, precursor pulsing order, ratio of dopant pulses) could be subject for optimization during the process. Hence the window/absorber interface of a solar cell could be freely tailored with optimal structural and/or electrical properties. The critical choice will be the choice of control parameters.

Acknowledgements

In media new discoveries always are presented as simple and readily available. As I first came to Uppsala I realized that R&D is far more complicated. Progress takes time and many ideas will never make it to the market or even to a scientific paper. Despite the technical and theoretical barriers though, I have acquired many skills of practical nature in the lab. The mutual attraction between broken equipment and me (or can it be pure coincidence?) perhaps did not always improve on the time schedule.

I would like to thank persons that meant a lot to me during this work:

My supervisor Lars Stolt. Working with you was a new experience. Among all projects and responsibilities every now and then you have found the time to check on my project and perhaps even run the machine. John Kessler who have guided me in some projects and around in Europe. I actually have learnt plenty about our continent from the English speaking Frenchman who drives a German car. The colleagues in the thin film solar cell group for all years in the lab and for providing me with CIGS! I also acknowledge senior researchers and students at the Hahn Meitner Institute with whom I worked during my stay in Berlin.

My corporate fellows, Johan, Jonas, Staffan, and Uppsala Holding. Maybe parental leave was not the best time possible to get into wireless business but the journey was worthwhile I think. Finally we passed the bankruptcy stage. Next project will be the big success! To Monika and Monica, my two Augusta sisters, and Anders. The third commitment maybe was third in priority but among the first of memories.

A greeting to all the stockholmers, with whom I've been car-pooling. You gave me many hours of interesting discussions, sometime half asleep though.

Professor Sören Berg and employees at the department of solid state electronics. Among you there is always a pleasant atmosphere with much laughter, at the laboratory and in the pist as well. A special greeting to all the old-guys (is anyone of you still employed?).

Klara and Jakob, you are the sunshine of my life!

Finally I thank Carola, my dear wife, who has given me all the love and support in the world during these years.

The Swedish Energy Agency, MISTRA, and the Swedish Institute are acknowledged for financial support.

Sollentuna, February 2004

Kadmiumfria buffertskikt för Cu(In,Ga)Se_2 solceller

En solcell kan beskrivas som en pn diod. Mellan områdena med olika ledningstyp bildas ett område utan rörliga laddningsbärare men med fasta laddade dopatomer. Dessa ger upphov till ett elektriskt fält som separerar elektroner och hål som bildats med energi från det inkommande ljuset. Det uppstår en spänning och en ström kan tas ut mellan p-sidan och n-sidan.

Den vanligaste typen av solceller är gjorda av kristallint kisel. För att fungera måste det vara högrent och kristallina kiselceller blir därför dyra. Dessutom är absorptionen låg och kiselceller måste därför göras relativt tjocka för att kunna fånga upp ljuset. Det finns halvledarmaterial som har högre absorption och kan användas till att göra tunnfilmssolceller. Ett sådant material är Cu(In,Ga)Se_2 (CIGS).

CIGS solceller använder vanligt fönsterglas som bärare. På glaset sputtras en bakkontakt av molybden. Sedan deponeras det ljusabsorberande CIGS skiktet genom samförångning av rena ämnen. Skiktet är ca 2 μm tjockt. På CIGS skiktet deponeras ett tunt buffertskikt med kadmiumsulfid (CdS) samt en framkontakt av zinkoxid (ZnO) för strömuppsamling. Själva pn övergången uppstår mellan CdS (n-dopat) och CIGS (p-dopat) skikten. För att undvika avfall med giftiga tungmetaller vid tillverkningen, är det önskvärt att ta fram ett Cd-fritt alternativ som buffertskikt. Det är ett komplext problem då man i dagsläget inte vet exakt vilken inverkan CdS skiktet och deponeringsprocessen har på solcellens prestanda. Det är känt att ett gränsskikt med låg kvalitet mellan buffert och CIGS ger ökade rekombinationsförluster. En lovande metod för att deponera Cd-fria buffertskikt är "Atomic layer deposition" (ALD). I denna avhandling undersöks buffertskikt av ZnO och In_2S_3 som är belagda med ALD samt vissa egenskaper hos gränsskiktet som bildas mellan dessa material och CIGS.

ALD är en metod för beläggning av enskilda atomlager. ZnO deponeras genom att växelvis införa pulser av dietylzink och vattenånga i en beläggningskammare. Enligt teorin begränsas ALD processen av ytmättade reaktioner. I detta arbete uppmärksammas avvikelser i filmtillväxten i ALD processen. Vid deponering av ZnO på CIGS förekommer problem med kärnbildning och processen påverkas negativt av föroreningar på CIGS ytan. I vilken grad tillväxten påverkas varierar med olika processkemikalier. Förekomsten av ytföroreningar är kopplad till ålder och till Na innehåll hos substratmaterialet. Förbättrad tillväxt har påvisats som resultat av olika förbehandlingar.

CIGS celler har tillverkats med buffertskikt av ZnO respektive In_2S_3. Det senare gav god verkningsgrad medan buffertskikt av ZnO fungerade sämre. Anpassningen mellan elektronenerginivåer hos buffert och absorbatorskikt anses vara bland de viktigaste parametrarna för att minimera verkningsgradsförluster i en solcell. Storleken på avståndet mellan valensbandet i CIGS och i buffertskiktet bestäms med hjälp av studier under vakuum med röntgen- och UV fotoelektronspektroskopi. Analysen utförs efter beläggning av ett antal atomlager. Enligt teorin bör steget i ledningsbandet vara litet men positivt för att optimera funktionen hos en solcell. Negativt ledningsbandssteg har mätts upp både för strukturen med ZnO på CIGS och med In_2S_3 på CIGS. Resultatet för In_2S_3 cellen är överraskande då ett negativt ledningsbandsteg antas resultera i ökade rekombinationsförluster.

En viktig aspekt vid användning av Cd-fria buffertskikt är passivering av CIGS ytan. En metod för passivering av yttillstånd är att värmebehandla CIGS skiktet i svavelväte, s.k. sulfurisering. Två processer för sulfurisering har undersökts. En vid lägre temperatur som syftar till att passivera samt en vid högre temperatur som har möjlighet att öka bandgapet i ytan av skiktet. Ett större bandgap kan reducera strömförluster pga rekombination i utarmningsområdet. Resultaten visar att sulfurisering vid hög temperatur endast ger fungerande solceller med Ga-fria absorbatorskikt. Ga-innehållande material gav låg verkningsgrad vilket kopplats till fas-separering i absorbatorskiktet. Sulfurisering vid låg temperatur gav förbättrade egenskaper för celler med ZnO-buffert vilket tyder på att processen har en passiverande effekt.

References

[1] M. A. Green, K. Emery, D. L. King, S. Igari, and W. Warta, *Solar cell efficiency tables (Version 22)*, Progress in Photovoltaics: Research and Applications **11** (5), (2003) 347.

[2] J. Kessler, M. Bodegård, J. Hedström, and L. Stolt, *Baseline Cu(In,Ca)Se_2 device production: control and statistical significance*, Solar Energy Materials and Solar Cells **67**, (2001) 67.

[3] K. Granath, Thesis, *The influence of Na on the growth of Cu(In,Ga)Se_2 layers for thin film solar cells*, Uppsala University, Uppsala (1999).

[4] M. A. Green, *Solar cells. Operating Principles, Technology and System Applications*. The University of New South Wales, Kensington, (1992).

[5] J. Kessler, J. Norling, O. Lundberg, J. Wennerberg, and L. Stolt, *Optimization of RF-sputtered ZnO/ZnO:Al for Cu(In,Ga)Se_2 based devices*, in Proceedings of the 16th European Photovoltaic Solar Energy Conference, Glasgow, (2000) 775.

[6] S. J. Fonash, *Solar Cell Device Physics*. Academic Press Inc., New York, (1981).

[7] S. M. Sze, *Physics of semiconductor devices*, 2nd ed. John Wiley & Sons, Inc., New York, (1981).

[8] T. Minemoto, T. Matsui, H. Takakura, Y. Hamakawa, T. Negami, Y. Hashimoto, T. Uenoyama, and M. Kitagawa, *Theoretical analysis of the effect of conduction band offset of window/CIS layers on performance of CIS solar cells using device simulation*, Solar Energy Materials and Solar Cells **67**, (2001) 83.

[9] G. B. Turner, R. J. Schwartz, and J. L. Gray, *Band discontinuity and bulk vs. interface recombination in CdS/CuInSe_2 solar cells*, in Proceedings of the 20th IEEE PV Specialist Conf, Las Vegas, (1988) 1457.

[10] Y. Hashimoto, K. Takeuchi, and K. Ito, *Band alignment at CdS/CuInS$_2$ heterojunction*, Applied Physics Letters **67** (7), (1995) 980.

[11] M. Morkel, L. Weinhardt, B. Lohmuller, C. Heske, E. Umbach, W. Riedl, S. Zweigart, and F. Karg, *Flat conduction-band alignment at the CdS/CuInS$_2$ thin-film solar-cell heterojunction*, Applied Physics Letters **79** (27), (2001) 4482.

[12] T. Löher, W. Jaegermann, and C. Pettenkofer, *Formation and Electronic-Properties of the CdS/CuInS$_2$(011) Heterointerface Studied by Synchrotron-Induced Photoemission*, Journal of Applied Physics **77** (2), (1995) 731.

[13] D. Schmid, M. Ruckh, F. Grunwald, and H.-W. Schock, *Chalcopyrite/defect chalcopyrite heterojunctions on the basis of CuInS$_2$*, Journal of Applied Physics **73** (6), (1993) 2902.

[14] L. L. Kazmerski, P. J. Ireland, F. R. White, and R. B. Cooper, *The performance of copper-ternary based thin-film solar cells*, in Proceedings of the 13th IEEE Photovoltaic Specialists Conference, Washington, (1978) 184.

[15] L. Kronik, L. Burstein, M. Leibovitch, Y. Shapira, D. Gal, E. Moons, J. Beier, G. Hodes, D. Cahen, D. Hariskos, R. Klenk, and H.-W. Schock,

Band diagram of the polycrystalline CdS/Cu(In,Ga)Se_2 heterojunction, Applied Physics Letters **67** (10), (1995) 1405.

16 T. Nakada, M. Hongo, and E. Hayashi, *Band offset of high efficiency CBD-ZnS/CIGS thin film solar cells*, Thin Solid Films **431-432**, (2003) 242.

17 C. Platzer-Björkman, J. Kessler, and L. Stolt, *Analysis of Zn(O,S) films for Cu(In,Ga)Se_2 solar cells*, in Proceedings of the Estonian Academy of Sciences. Physics. Mathematics., Tartu, (2003) 299.

18 A. J. Nelson, C. R. Schwerdtfeger, S.-H. Wei, A. Zunger, D. Rioux, R. Patel, and H. Hochst, *Theoretical and experimental studies of the ZnSe/CuInSe_2 heterojunction band offset*, Applied Physics Letters **62** (20), (1993) 2557.

19 J. Kessler, M. Ruckh, D. Hariskos, U. Ruhle, R. Menner, and H. W. Schock, *Interface engineering between CuInSe_2 and ZnO*, in Proceedings of the 23rd IEEE Photovoltaic Specialists Conference, (1993) 447.

20 D. Lincot, J. F. Guillemoles, P. Cowache, A. Marlot, B. Lepiller, B. Canava, E. B. Yousfi, and J. Vedel, *Solution deposition technologies for thin film solar cells: status and perspectives*, in Proceedings of the 2nd World Conference on Photovoltaic Energy Conversion, Vienna, (1998) 440.

21 J. Kessler, K.-O. Velthaus, M. Ruckh, R. Laichinger, and H.-W. Schock, *Chemical bath deposition of CdS on CuInSe_2, etching effects and growth kinetics*, in Proceedings of the 6th International Photovoltaic Science and Engineering Conference, New Delhi, India, (1992) 1005.

22 T. Wada, *Microstructural characterization of high-efficiency Cu(In,Ga)Se_2 solar cells*, Solar Energy Materials and Solar Cells **49** (1-4), (1997) 249.

23 T. Nakada and A. Kunioka, *Direct evidence of Cd diffusion into Cu(In,Ga)Se_2 thin films during chemical-bath deposition process of CdS films*, Applied Physics Letters **74** (17), (1999) 2444.

24 K. Ramanathan, R. N. Bhattacharya, J. E. Granata, J. Webb, D. W. Niles, M. A. Contreras, H. Wiesner, F. S. Hasoon, and R. Noufi, *Advances in the CIS research at NREL*, in Proceedings of the 26th IEEE Photovoltaic Specialists Conference, (1997) 319.

25 T. Nakada, K. Furumi, and A. Kunioka, *High-efficiency cadmium-free Cu(In,Ga)Se_2 thin-film solar cells with chemically deposited ZnS buffer layers*, IEEE Transactions on Electron Devices **46** (10), (1999) 2093.

26 S. Chaisitsak, A. Yamada, and M. Konagai, *Comprehensive study of light-soaking effect in ZnO/Cu(InGa)Se_2 solar cells with Zn-based buffer layers*, in Proceedings of the II-VI Compound Semiconductor Photovoltaic Materials Symposium, (2001)

27 R. Herberholz, M. Igalson, and H. W. Schock, *Distinction between bulk and interface states in CuInSe_2/Cd/ZnO by space charge spectroscopy*, Journal of Applied Physics **83** (1), (1998) 318.

28 P. Zabierowski, M. Igalson, and H. W. Schock, *Light-induced metastabilities in the interface region of Cu(In,Ga)Se_2-based photovoltaic devices studied by Laplace transform junction spectroscopy*, Solid State Phenomena **67-8**, (1999) 403.

[29] K. Orgassa, U. Rau, Q. Nguyen, H. W. Schock, and J. H. Werner, *Role of the CdS buffer layer as an active optical element in Cu(In,Ga)Se_2 thin-film solar cells*, Progress in Photovoltaics: Research and Applications **10** (7), (2002) 457.

[30] T. Suntola, in *Handbook of Crystal Growth*, edited by D.T.J. Hurle (North-Holland Elsevier Science Publishers, Amsterdam, 1994), Vol. 3, pp. 605.

[31] M. Juppo, M. Vehkamaki, M. Ritala, and M. Leskela, *Deposition of molybdenum thin films by an alternate supply of $MoCl_5$ and Zn*, Journal of Vacuum Science & Technology A **16** (5), (1998) 2845.

[32] H. Otoma, T. Honda, K. Hara, J. Yoshino, and H. Kukimoto, *Growth of $CuGaS_2$ by Alternating-Source-Feeding MOVPE*, Journal of Crystal Growth **115** (1-4), (1991) 807.

[33] H.-S. Park, J.-S. Min, J.-W. Lim, and S.-W. Kang, *Theoretical evaluation of film growth rate during atomic layer epitaxy*, Applied Surface Science **158**, (2000) 81.

[34] T. Suntola, *Surface chemistry of materials deposition at atomic layer level*, Applied Surface Science **100-101**, (1996) 391.

[35] L. C. Olsen, P. Eschbach, and S. Kundu, *Role of buffer layers in CIS-based solar cells*, in Proceedings of the 29th IEEE Photovoltaic Specialists Conference, New York, (2002) 652.

[36] V. Lujala, J. Skarp, M. Tammenmaa, and T. Suntola, *Atomic layer epitaxy growth of doped zinc oxide thin films from organometals*, Applied Surface Science **82-83**, (1994) 34.

[37] L. Stolt, J. Hedström, and J. Skarp, *CIS Solar Cells with ZnO Windows Deposited by ALE*, in Proceedings of the 1st World Conference on Photovoltaic Energy Conversion, Hawaii, (1994) 250.

[38] A. Shimizu, S. Chaisitsak, T. Sugiyama, A. Yamada, and M. Konagai, *Zinc-based buffer layer in the Cu(InGa)Se_2 thin film solar cells*, Thin Solid Films **361-362**, (2000) 193.

[39] L. C. Olsen, W. H. Lei, F. W. Addis, W. N. Shafarman, M. A. Contreras, and K. Ramanathan, *High efficiency CIGS and CIS cells with CVD ZnO buffer layers*, in Proceedings of the 26th IEEE Photovoltaic Specialists Conference, Anaheim, (1997) 363.

[40] A. Yamada, B. Sang, and M. Konagai, *Atomic layer deposition of ZnO transparent conducting oxides*, Applied Surface Science **112**, (1997) 216.

[41] J. Skarp, 5th techncal report on the contribution of Microchemistry Ltd. in the Eurocis-project. Contract number JOU2-CT92-0141, (1995).

[42] E. B. Yousfi, B. Weinberger, F. Donsanti, P. Cowache, and D. Lincot, *Atomic layer deposition of zinc oxide and indium sulfide layers for Cu(In,Ga)Se_2 thin-film solar cells*, Thin Solid Films **387**, (2001) 29.

[43] T. Minami, H. Sonohara, S. Takata, and I. Fukuda, *Low temperature formation of textured ZnO transparent electrodes by magnetron sputtering*, Journal of Vacuum Science & Technology A: Vacuum, Surfaces, and Films **13** (3 pt 1), (1995) 1053.

[44] C. Platzer-Björkman, J. Kessler, and L. Stolt, *Atomic layer deposition of Zn(O,S) buffer layers for high efficiency Cu(In,Ga)Se_2 solar cells*, to

appear in Proceedings of the 3rd World Conference on Photovoltaic Energy Conversion, Osaka, (2003)

[45] Y. Ohtake, K. Kushiya, M. Ichikawa, A. Yamada, and M. Konagai, *Polycrystalline Cu(InGa)Se_2 thin-film solar cells with ZnSe buffer layers*, Japanese Journal of Applied Physics **34** (11), (1995) 5949.

[46] N. Naghavi, S. Spiering, M. Powalla, B. Cavana, and D. Lincot, *High-efficiency copper indium gallium diselenide (CIGS) solar cells with indium sulfide buffer layers deposited by atomic layer chemical vapor deposition (ALCVD)*, Progress in Photovoltaics **11** (7), (2003) 437.

[47] E. B. Yousfi, T. Asikainen, V. Pietu, P. Cowache, M. Powalla, and D. Lincot, *Cadmium-free buffer layers deposited by atomic later epitaxy for copper indium diselenide solar cells*, Thin Solid Films **361-362**, (2000) 183.

[48] J.-F. Guillemoles, B. Canava, E. B. Yousfi, P. Cowache, A. Galtayries, T. Asikainen, M. Powalla, D. Hariskos, H.-W. Schock, and D. Lincot, *Indium-based interface chemical engineering by electrochemistry and atomic layer deposition for copper indium diselenide solar cells*, Japanese Journal of Applied Physics **40**, (2001) 6065.

[49] N. Barreau, J. C. Bernede, S. Marsillac, C. Amory, and W. N. Shafarman, *New Cd-free buffer layer deposited by PVD: In_2S_3 containing Na compounds*, Thin Solid Films **431-432**, (2003) 326.

[50] N. Barreau, J. C. Bernede, and S. Marsillac, *Study of the new beta -In_2S_3 containing Na thin films. II. Optical and electrical characterization of thin films*, Journal of Crystal Growth **241**, (2002) 51.

[51] C. Platzer-Björkman, J. Lu, J. Kessler, and L. Stolt, *Interface study of $CuInSe_2$/ZnO and Cu(In,Ga)Se_2/ZnO devices using ALD ZnO buffer layers*, Thin Solid Films **431-432**, (2003) 321.

[52] M. Ruckh, D. Schmid, M. Kaiser, R. Schaffler, T. Walter, and H. W. Schock, *Influence of substrates on the electrical properties of Cu(In,Ga)Se_2 thin films*, Solar Energy Materials and Solar Cells **41-2**, (1996) 335.

[53] L. Kronik, D. Cahen, and H. W. Schock, *Effects of sodium on polycrystalline Cu(In,Ga)Se_2 and its solar cell performance*, Advanced Materials **10**, (1998) 31.

[54] D. Cahen and R. Noufi, *Defect chemical explanation for the effect of air anneal on CdS/$CulnSe_2$ solar cell performance*, Applied Physics Letters **54**, (1989) 558.

[55] R. Scheer, *Surface and interface properties of Cu-chalcopyrite semiconductors and devices*, Trends in Vacuum Science and Technology **2**, (1997) 77.

[56] M. Bodegård, L. Stolt, and J. Hedström, *The influence of sodium on the grain structure of $CuInSe_2$ films for photovoltaic applications*, in Proceedings of the 12th European Photovoltaic Solar Energy Conference, Amsterdam, (1994) 1743.

[57] M. Bodegård, Thesis, *Growth of $CuInSe_2$ and Cu(In,Ga)Se_2 thin films for solar cells*, Royal Institute of Technology, Stockholm (1996).

[58] A. Kylner, *The chemical bath deposited CdS/Cu(In,Ga)Se_2 interface as revealed by X-ray photoelectron spectroscopy*, Journal of the Electrochemical Society **146** (5), (1999) 1816.

[59] L. Stolt and M. Bodegård, *High efficiency thin film solar cells based on chalcopyrite semiconductors*, Crystal Research Technology **31**, (1995) 397.

[60] D. Briggs and M. P. Seah, *Practical Surface Analysis*. Wiley, (1990).

[61] V. Lyahovitskaya, Y. Feldman, K. Gartsman, H. Cohen, C. Cytermann, and D. Cahen, *Na effects on $CuInSe_2$: Distinguishing bulk from surface phenomena*, Journal of Applied Physics **91**, (2002) 4205.

[62] J. F. Moulder, W. F. Stickle, P. E. Sobol, and K. D. Bomben, *Handbook of X-ray Photoelectron Spectroscopy*. Physical Electronics, Inc., (1995).

[63] T. Sugiyama, S. Chaisitsak, A. Yamada, M. Konagai, Y. Kudriavtsev, A. Godines, A. Villegas, and R. Asomoza, *Formation of pn homojunction in Cu(InGa)Se_2 thin film solar cells by Zn doping*, Japanese Journal of Applied Physics **39**, (2000) 4816.

[64] E. B. Yousfi, J. Fouache, and D. Lincot, *Study of atomic layer epitaxy of zinc oxide by in-situ quartz crystal microgravimetry*, Applied Surface Science **153** (4), (2000) 223.

[65] K. Kukli, J. Arik, A. Aidla, H. Siimon, M. Ritala, and M. Leskelä, *In situ study of atomic layer epitaxy growth of tantalum oxide thin films from $Ta(OC_2H_5)_5$ and H_2O*, Applied Surface Science **112**, (1997) 236.

[66] A. Rosental, P. Adamson, A. Gerst, and A. Niilisk, *Monitoring of atomic layer deposition by incremental dielectric reflection*, Applied Surface Science **107**, (1996) 178.

[67] M. Ritala, M. Juppo, K. Kukli, A. Rahtu, and M. Leskelä, *In situ characterization of atomic layer deposition processes by a mass spectrometer*, Journal de Physique IV **9** (8), (1999) 1021.

[68] R. G. v. Welzenis, R. A. M. Bink, and H. H. Brongersma, *A mini-ALE attachment to UHV surface analysis equipment*, Applied Surface Science **107**, (1996) 255.

[69] S.-H. Wei and A. Zunger, *Band offsets and optical bowings of chalcopyrites and Zn-based II-VI alloys*, Journal of Applied Physics **78** (6), (1995) 3846.

[70] O. Lundberg, Thesis, *Band gap profiling and high speed deposition of Cu(In,Ga)Se_2 for thin film solar cells*, Uppsala University, Uppsala (2003).

[71] T. Walter, R. Menner, C. Köble, and H. W. Schock, *Characterization and junction performance of highly efficient ZnO/CdS/$CuInS_2$ thin film solar cells*, in Proceedings of the 12th EC Photovoltaic Solar Energy Conference, Amsterdam, (1994) 1755.

[72] J. R. Tuttle, J. R. Sites, A. Delahoy, W. N. Shafarman, B. Basol, S. Fonash, J. Gray, R. Menner, J. Phillips, A. Rockett, J. Scofield, F. R. Shapiro, P. Singh, V. Suntharalingam, D. Tarrant, T. Walter, S. Wiedeman, and T. M. Peterson, *Characterization and modeling of Cu(In, Ga)(S, $Se)_2$-based photovoltaic devices: a laboratory and industrial perspective*, Progress in Photovoltaics: Research and Applications **3**, (1995) 89.

[73] W. N. Shafarman, J. Titus, M. Haimbodi, G. Gossla, S. Hanket, S. Marsillac, and T. Minemoto, *Advances in $CuInSe_2$-based Solar Cells: From Fundamentals to Processing*, in Proceedings of the NCPV and Solar program review meeting, (2003) 1.

[74] I. M. Kötschau, M. Turcu, U. Rau, and H. W. Schock, *Structural and electronic properties of polycrystalline $Cu(In,Ga)(S,Se)_2$ alloys*, in Proceedings of the II-VI Compound Semiconductor Photovoltaic Materials Symposium, (2001)

[75] J. J. M. Binsma and V. d. L. H.A., *Preparation of thin $CuInS_2$ films via a two-stage process*, Thin Solid Films **97**, (1982) 237.

[76] V. Probst, F. Karg, J. Rimmasch, F. Riedl, W. Stetter, Harm, and O. Eibl, *Advanced Stacked Elemental Layer Process for $Cu(In,Ga)Se_2$ Thin Film Photovoltaic Devices*, in Proceedings of the Material Research Society Symposium, San Fransisco, (1996) 165.

[77] Y. Nagoya, K. Kushiya, M. Tachiyuki, and O. Yamase, *Role of incorporated sulfur into the surface of $Cu(InGa)Se_2$ thin-film absorber*, Solar Energy Materials and Solar Cells **67**, (2001) 247.

[78] T. Nakada, H. Ohbo, T. Watanabe, H. Nakazawa, M. Matsui, and A. Kunioka, *Improved $Cu(In,Ga)(S,Se)_2$ thin film solar cells by surface sulfurization*, Solar Energy Materials and Solar Cells **49**, (1997) 285.

[79] D. Ohashi, T. Nakada, and A. Kunioka, *Improved CIGS thin-film solar cells by surface sulfurization using In_2S_3 and sulfur vapor*, Solar Energy Materials and Solar Cells **67**, (2001) 261.

[80] C. L. Jensen, D. E. Tarrant, J. H. Ermer, and G. A. Pollock, *The role of gallium in $CuInSe_2$ solar cells fabricated by a two-stage method*, in Proceedings of the 23rd IEEE Photovoltaic Specialists Conference, Louisville, KY, USA, (1993) 577.

Acta Universitatis Upsaliensis

Comprehensive Summaries of Uppsala Dissertations from the Faculty of Science and Technology

Editor: The Dean of the Faculty of Science and Technology

A doctoral dissertation from the Faculty of Science and Technology, Uppsala University, is usually a summary of a number of papers. A few copies of the complete dissertation are kept at major Swedish research libraries, while the summary alone is distributed internationally through the series *Comprehensive Summaries of Uppsala Dissertations from the Faculty of Science and Technology*. (Prior to October, 1993, the series was published under the title "Comprehensive Summaries of Uppsala Dissertations from the Faculty of Science".)

Distribution:
Uppsala University Library
Box 510, SE-751 20 Uppsala, Sweden
www.uu.se, acta@ub.uu.se

ISSN 1104-232X
ISBN 91-554-5883-1